7. Dantas JR Jr, Okuno Y, Asada H, Tamura M, Takahashi M, Tanishita O, Takahashi Y, Kurata T, Yamanishi K (1986) Characterization of glycoproteins of viruses causing hemorrhagic fever with renal syndrome (HFRS) using monoclonal antibodies. Virology 151:379–384
8. Dzagurova T, Tkachenko E, Slonova R, Ivanov L, Ivanidze E, Markeshin S, Dekonenko A, Niklasson B, Lundkvist A (1995) Antigenic relationships of hantavirus strains analysed by monoclonal antibodies. Arch Virol 140:1763–1773
9. Elgh F, Wadell G, Juto P (1995) Comparison of the kinetics of Puumala virus specific IgM and IgG antibody responses in nephropathia epidemica as measured by a recombinant antigen-based enzyme-linked immunosorbent assay and an immunofluorescence test. J Med Virol 45:146–150
10. Franko MC, Gibbs CJ Jr, Lee PW, Gajdusek DC (1983) Monoclonal antibodies specific for Hantaan virus. P Natl Acad Sci USA 80:4149–4153
11. Jonsson CB, Schmaljohn CS (2001) Replication of hantaviruses. Curr Top Microbiol Immunol 256:15–32
12. Kang HJ, Arai S, Hope AG, Song JW, Cook JA, Yanagihara R (2009) Genetic diversity and phylogeography of Seewis virus in the Eurasian common shrew in Finland and Hungary. Virol J 6:208
13. Kang HJ, Arai S, Hope AG, Cook JA, Yanagihara R (2010) Novel hantavirus in the flat-skulled shrew (Sorex roboratus). Vector Borne Zoonotic Dis 10:593–597
14. Kang HJ, Bennett SN, Hope AG, Cook JA, Yanagihara R (2011) Shared ancestry between a newfound mole-borne hantavirus and hantaviruses harbored by cricetid rodents. J Virol 85(15):7496–7503
15. Klempa B, Fichet-Calvet E, Lecompte E, Auste B, Aniskin V, Meisel H, Denys C, Koivogui L, ter Meulen J, Kruger DH (2006) Hantavirus in African wood mouse, Guinea. Emerg Infect Dis 12:838–840
16. Klempa B, Fichet-Calvet E, Lecompte E, Auste B, Aniskin V, Meisel H, Barriere P, Koivogui L, ter Meulen J, Kruger DH (2007) Novel hantavirus sequences in Shrew, Guinea. Emerg Infect Dis 13:520–522
17. Koch J, Liang MF, Queitsch I, Kraus AA, Bautz EKF (2003) Human recombinant neutralizing antibodies against Hantaan virus G2 protein. Virology 308:64–73
18. Kucinskaite-Kodze I, Petraityte-Burneikiene R, Zvirbliene A, Hjelle B, Medina RA, Gedvilaite A, Razanskiene A, Schmidt-Chanasit J, Mertens M, Padula P, Sasnauskas K, Ulrich RG (2011) Characterization of monoclonal antibodies against hantavirus nucleocapsid protein and their use for immunohistochemistry on rodent and human samples. Arch Virol 156:443–456
19. Liang M, Guttieri M, Lundkvist A, Schmaljohn C (1997) Baculovirus expression of a human G2-specific, neutralizing IgG monoclonal antibody to Puumala virus. Virology 235:252–260
20. Liang M, Mahler M, Koch J, Ji Y, Li D, Schmaljohn C, Bautz EK (2003) Generation of an HFRS patient-derived neutralizing recombinant antibody to Hantaan virus G1 protein and definition of the neutralizing domain. J Med Virol 69:99–107
21. Lundkvist A, Fatouros A, Niklasson B (1991) Antigenic variation of European haemorrhagic fever with renal syndrome virus strains characterized using bank vole monoclonal antibodies. J Gen Virol 72(Pt 9):2097–2103
22. Lundkvist A, Niklasson B (1992) Bank vole monoclonal antibodies against Puumala virus envelope glycoproteins: identification of epitopes involved in neutralization. Arch Virol 126:93–105
23. Lundkvist A, Horling J, Athlin L, Rosen A, Niklasson B (1993) Neutralizing human monoclonal antibodies against Puumala virus, causative agent of nephropathia epidemica: a novel method using antigen-coated magnetic beads for specific B cell isolation. J Gen Virol 74(Pt 7):1303–1310
24. Lundkvist A, Vapalahti O, Plyusnin A, Sjolander KB, Niklasson B, Vaheri A (1996) Characterization of Tula virus antigenic determinants defined by monoclonal antibodies raised against baculovirus-expressed nucleocapsid protein. Virus Res 45:29–44
25. Lundkvist A, Meisel H, Koletzki D, Lankinen H, Cifire F, Geldmacher A, Sibold C, Gott P, Vaheri A, Kruger DH, Ulrich R (2002) Mapping of B-cell epitopes in the nucleocapsid protein of Puumala hantavirus. Viral Immunol 15:177–192
26. Mazzarotto GA, Raboni SM, Stella V, Carstensen S, de Noronha L, Levis S, Zanluca C, Zanetti CR, Bordignon J, Duarte dos Santos CN (2009) Production and characterization of monoclonal antibodies against the recombinant nucleoprotein of Araucaria hantavirus. J Virol Methods 162:96–100
27. Mertens M, Hofmann J, Petraityte-Burneikiene R, Ziller M, Sasnauskas K, Friedrich R, Niederstrasser O, Kruger DH, Groschup MH, Petri E, Werdermann S, Ulrich RG (2011) Seroprevalence study in forestry workers of a non-endemic region in eastern Germany reveals infections by Tula and Dobrava-Belgrade hantaviruses. Med Microbiol Immunol 200:263–268
28. Mertens M, Kindler E, Emmerich P, Esser J, Wagner-Wiening C, Wolfel R, Petraityte-Burneikiene R, Schmidt-Chanasit J, Zvirbliene A, Groschup MH, Dobler G, Pfeffer M, Heckel G, Ulrich RG, Essbauer SS (2011) Phylogenetic analysis of Puumala virus subtype Bavaria, characterization and diagnostic use of its recombinant nucleocapsid protein. Virus Genes
29. Motokawa M, Suzuki H, Harada M, Lin L-K, Koyasu K, S-I Oda (2000) Phylogenetic relationships among East Asian species of Crocidura (Mammalia, Insectivora) inferred from mitochondrial cytochrome b gene sequences. Zoological Sci (Tokyo) 17: 497–504
30. Okumura M, Yoshimatsu K, Kumperasart S, Nakamura I, Ogino M, Taruishi M, Sungdee A, Pattamadilok S, Ibrahim IN, Erlina S, Agui T, Yanagihara R, Arikawa J (2007) Development of serological assays for Thottapalayam virus, an insectivore-borne Hantavirus. Clin Vaccine Immunol 14:173–181
31. Plyusnin A, Morzunov SP (2001) Virus evolution and genetic diversity of hantaviruses and their rodent hosts. Curr Top Microbiol Immunol 256:47–75
32. Ramsden C, Holmes EC, Charleston MA (2009) Hantavirus evolution in relation to its rodent and insectivore hosts: no evidence for codivergence. Mol Biol Evol 26:143–153
33. Razanskiene A, Schmidt J, Geldmacher A, Ritzi A, Niedrig M, Lundkvist A, Kruger DH, Meisel H, Sasnauskas K, Ulrich R (2004) High yields of stable and highly pure nucleocapsid proteins of different hantaviruses can be generated in the yeast Saccharomyces cerevisiae. J Biotechnol 111:319–333
34. Ruo SL, Sanchez A, Elliott LH, Brammer LS, McCormick JB, Fisher-Hoch SP (1991) Monoclonal antibodies to three strains of hantaviruses: Hantaan, R22, and Puumala. Arch Virol 119:1–11
35. Salonen EM, Parren PW, Graus YF, Lundkvist A, Fisicaro P, Vapalahti O, Kallio-Kokko H, Vaheri A, Burton DR (1998) Human recombinant Puumala virus antibodies: cross-reaction with other hantaviruses and use in diagnostics. J Gen Virol 79(Pt 4):659–665
36. Schmidt-Chanasit J, Essbauer S, Petraityte R, Yoshimatsu K, Tackmann K, Conraths FJ, Sasnauskas K, Arikawa J, Thomas A, Pfeffer M, Scharninghausen JJ, Splettstoesser W, Wenk M, Heckel G, Ulrich RG (2010) Extensive host sharing of central European Tula virus. J Virol 84:459–474
37. Schlegel M, Radosa L, Rosenfeld UM, Schmidt S, Triebenbacher C, Löhr PW, Fuchs D, Heroldová M, Jánová E, Stanko M, Mošanský L, Fričová J, Pejčoch M, Suchomel J, Purchart L, Groschup MH, Krüger DH, Klempa B, Ulrich RG (2012) Broad geographical distribution and high genetic diversity of shrew-borne Seewis hantavirus in Central Europe. Virus Genes [Epub ahead of print]

38. Song JW, Baek LJ, Schmaljohn CS, Yanagihara R (2007) Thottapalayam virus, a prototype shrewborne hantavirus. Emerg Infect Dis 13:980–985
39. Song JW, Gu SH, Bennett SN, Arai S, Puorger M, Hilbe M, Yanagihara R (2007) Seewis virus, a genetically distinct hantavirus in the Eurasian common shrew (Sorex araneus). Virol J 4:114
40. Song JW, Kang HJ, Gu SH, Moon SS, Bennett SN, Song KJ, Baek LJ, Kim HC, O'Guinn ML, Chong ST, Klein TA, Yanagihara R (2009) Characterization of Imjin virus, a newly isolated hantavirus from the Ussuri white-toothed shrew (Crocidura lasiura). J Virol 83:6184–6191
41. Sugiyama K, Morikawa S, Matsuura Y, Tkachenko EA, Morita C, Komatsu T, Akao Y, Kitamura T (1987) Four serotypes of haemorrhagic fever with renal syndrome viruses identified by polyclonal and monoclonal antibodies. J Gen Virol 68(Pt 4): 979–987
42. Tischler ND, Rosemblatt M, Valenzuela PD (2008) Characterization of cross-reactive and serotype-specific epitopes on the nucleocapsid proteins of hantaviruses. Virus Res 135:1–9
43. Yadav PD, Vincent MJ, Nichol ST (2007) Thottapalayam virus is genetically distant to the rodent-borne hantaviruses, consistent with its isolation from the Asian house shrew (Suncus murinus). Virol J 4:80
44. Yamada T, Hjelle B, Lanzi R, Morris C, Anderson B, Jenison S (1995) Antibody responses to Four Corners hantavirus infections in the deer mouse (Peromyscus maniculatus): identification of an immunodominant region of the viral nucleocapsid protein. J Virol 69:1939–1943
45. Yamanishi K, Dantas JR Jr, Takahashi M, Yamanouchi T, Domae K, Takahashi Y, Tanishita O (1984) Antigenic differences between two viruses, isolated in Japan and Korea, that cause hemorrhagic fever with renal syndrome. J Virol 52:231–237
46. Yashina LN, Abramov SA, Gutorov VV, Dupal TA, Krivopalov AV, Panov VV, Danchinova GA, Vinogradov VV, Luchnikova EM, Hay J, Kang HJ, Yanagihara R (2010) Seewis virus: phylogeography of a shrew-borne hantavirus in Siberia, Russia. Vector Borne Zoonotic Dis 10:585–591
47. Yoshimatsu K, Arikawa J, Kariwa H (1993) Application of a recombinant baculovirus expressing hantavirus nucleocapsid protein as a diagnostic antigen in IFA test: cross reactivities among 3 serotypes of hantavirus which causes hemorrhagic fever with renal syndrome (HFRS). J Vet Med Sci 55:1047–1050
48. Yoshimatsu K, Arikawa J, Yoshida R, Li H, Yoo YC, Kariwa H, Hashimoto N, Kakinuma M, Nobunaga T, Azuma I (1995) Production of recombinant hantavirus nucleocapsid protein expressed in silkworm larvae and its use as a diagnostic antigen in detecting antibodies in serum from infected rats. Lab Anim Sci 45:641–646
49. Yoshimatsu K, Arikawa J, Tamura M, Yoshida R, Lundkvist A, Niklasson B, Kariwa H, Azuma I (1996) Characterization of the nucleocapsid protein of Hantaan virus strain 76–118 using monoclonal antibodies. J Gen Virol 77(Pt 4):695–704
50. Yu S, Liang M, Fan B, Xu H, Li C, Zhang Q, Li D, Tang B, Li S, Dai Y, Wang M, Zheng M, Yan B, Zhu Q, Li N (2006) Maternally derived recombinant human anti-hantavirus monoclonal antibodies are transferred to mouse offspring during lactation and neutralize virus in vitro. J Virol 80:4183–4186
51. Zoller LG, Yang S, Gott P, Bautz EK, Darai G (1993) A novel mucapture enzyme-linked immunosorbent assay based on recombinant proteins for sensitive and specific diagnosis of hemorrhagic fever with renal syndrome. J Clin Microbiol 31:1194–1199
52. Zvirbliene A, Samonskyte L, Gedvilaite A, Voronkova T, Ulrich R, Sasnauskas K (2006) Generation of monoclonal antibodies of desired specificity using chimeric polyomavirus-derived virus-like particles. J Immunol Methods 311:57–70

Journal of Virological Methods 185 (2012) 74–81

Contents lists available at SciVerse ScienceDirect

Journal of Virological Methods

journal homepage: www.elsevier.com/locate/jviromet

Development of a serotyping enzyme-linked immunosorbent assay system based on recombinant truncated hantavirus nucleocapsid proteins for New World hantavirus infection

Takaaki Koma[a], Kumiko Yoshimatsu[a], Midori Taruishi[a,1], Daisuke Miyashita[b], Rika Endo[a], Kenta Shimizu[a], Shumpei P. Yasuda[a], Takako Amada[a], Takahiro Seto[b], Ryo Murata[b], Haruka Yoshida[b], Hiroaki Kariwa[b], Ikuo Takashima[b], Jiro Arikawa[a,*]

[a] Department of Microbiology, Graduate School of Medicine, Hokkaido University, Kita-ku, Kita-15, Nishi-7, Sapporo 060-8638, Japan
[b] Laboratory of Public Health, Graduate School of Veterinary Medicine, Hokkaido University, Kita-ku, Kita-18, Nishi 9, Sapporo 060-0818, Japan

Article history:
Received 13 February 2012
Received in revised form 1 June 2012
Accepted 11 June 2012
Available online 18 June 2012

Keywords:
Hantavirus
Hantavirus pulmonary syndrome
Serotyping
ELISA
Nucleocapsid protein

A B S T R A C T

New World hantaviruses were divided into five groups based on the amino acid sequence variability of the internal variable region (around 230–302 amino acids) of hantavirus nucleocapsid protein (NP). Sin Nombre virus (SNV), Andes virus, Black Creek Canal virus (BCCV), Carrizal virus (CARV) and Cano Delgadito virus belong to groups 1, 2, 3, 4 and 5, respectively. Patient and rodent sera were serotyped successfully by an enzyme-linked immunosorbent assay (ELISA) with recombinant truncated NP lacking 99 N-terminal amino acids (trNP100) of SNV, CARV and BCCV. The trNP100 of BCCV showed lower reactivity to heterologous sera. In contrast, whole recombinant NP antigens detected both homologous and heterologous antibodies equally. The results together with results of a previous study suggest that trNP100 can distinguish infections among viruses in groups 1, 2, 3 and 4 of New World hantaviruses. The serotyping ELISA with trNP100 is useful for epidemiological surveillance in humans and rodents.
© 2012 Elsevier B.V. All rights reserved.

1. Introduction

Hantaviruses belong to the family *Bunyaviridae* and are maintained in rodents and other small mammals that are infected persistently (Schmaljohn and Hjelle, 1997). Hantaviruses cause two febrile illnesses in humans, hemorrhagic fever with renal syndrome (HFRS) in the Old World and hantavirus pulmonary syndrome (HPS) in the New World (Kariwa et al., 2007; Schmaljohn and Hjelle, 1997). Transmission of the viruses to humans occurs through inhalation of aerosolized animal excreta or rodent bites (Lee and van der Groen, 1989; Meyer and Schmaljohn, 2000). Hantaviruses appear to have co-evolved with the rodent reservoir host species over many thousands of years (Hughes and Friedman, 2000; Schmaljohn and Hjelle, 1997). The difference in epidemic areas of HFRS and HPS depends on the rodent habitat (Zeier et al., 2005).

Hantavirus virions contain three segmented negative-sense RNAs designated S, M, L; they encode a nucleocapsid protein (NP), enveloped glycoproteins (Gn and Gc), and an RNA-dependent RNA polymerase (L protein), respectively (Elliott, 1990; Schmaljohn, 1996). Hantavirus NP is the most abundant viral component in both virions and infected cells and can form a stable trimer (Elliott et al., 2000; Kaukinen et al., 2001, 2004). The NP of hantaviruses possesses immunodominant, linear, cross-reactive epitopes around the first 100 amino acids (aa) of the N-terminus (Elgh et al., 1996; Gott et al., 1997; Vapalahti et al., 1995; Yamada et al., 1995). On the other hand, the variable region around 230–302 aa forms serotype-specific epitopes after multimerization of NP (Tischler et al., 2008; Yoshimatsu et al., 2003).

Recombinant antigens were expressed with multimerization-dependent serotype-specific epitopes after truncation of the N-terminal 49 aa in NP (trNP50) by a baculovirus (Araki et al., 2001; Nakamura et al., 2008; Yasuda et al., 2012). Enzyme-linked immunosorbent assay (ELISA) using trNP50 differentiated successfully infections with four different serotypes of Old World hantavirus: Hantaan, Seoul, Dobrava, and Thailand viruses in HFRS patient and rodent sera (Araki et al., 2001; Nakamura et al., 2008). ELISA using trNP lacking 99 aa of the N-terminal end of the NP (trNP100) differentiated successfully infections with three different serotypes of New World hantaviruses: Sin Nombre virus (SNV), Andes virus (ANDV) and Laguna Negra virus (LANV) in HPS patient and rodent sera (Koma et al., 2010). Therefore, the serotyping ELISA using trNPs is a more rapid, safe and simple method as a substitute

* Corresponding author. Tel.: +81 11 706 6905; fax: +81 11 706 7879.
E-mail address: j_arika@med.hokudai.ac.jp (J. Arikawa).
[1] Present address: Department of Molecular Virology and Microbiology, Baylor College of Medicine, One Baylor Plaza, Houston, TX 77030, USA.

0166-0934/$ – see front matter © 2012 Elsevier B.V. All rights reserved.
http://dx.doi.org/10.1016/j.jviromet.2012.06.006

for the neutralization test, which has been the only serological assay for determining the serotype (Araki et al., 2001; Koma et al., 2010; Nakamura et al., 2008).

Since the first recognition of HPS in the United States in 1993, more than 30 new hantaviral strains or genetic lineages have been identified from patients with HPS or various rodent species throughout the Americas (Jonsson et al., 2010; Peters and Khan, 2002; Schmaljohn and Hjelle, 1997). However, the antigenic relationship among the New World hantaviruses has not been studied in detail.

Since serotyping with trNP depended on the antigenic difference of serotype-specific epitopes within the internal region of trNP, it was expected that variability of the aa sequences in the region also correlated to the hantavirus serotype. In the present study, therefore, amino acid sequences of the internal variable regions of NP of many New World hantaviruses were compared. The results showed that they were divided into 5 groups. Therefore, SNV (group 1) and Black Creek Canal virus (BCCV) (group 3), which were associated with HPS in the United States (Hjelle et al., 1994; Ravkov et al., 1995), and Carrizal virus (CARV) (group 4), which was recognized recently as a New World hantavirus isolated from *Reithrodontomys sumichrasti* in Mexico (Kariwa et al., 2012), were selected, and the applicability of their trNPs for a serotyping antigen was examined.

2. Materials and methods

2.1. cDNAs

cDNAs containing coding information for the S segment of SNV strain SN 77734 (Botten et al., 2000), CARV strain 2/2006 (Kariwa et al., 2012) and BCCV (GenBank ID: AB689163) were used. CARV was recognized recently from *R. sumichrasti* in Mexico (Kariwa et al., 2012).

2.2. Monoclonal antibodies and human and rodent sera

Monoclonal antibodies (MAbs) to the NP of HTNV and PUUV were used for antigenic characterization of the NP by an indirect immunofluorescence assay (IFA). The MAbs 2E12, 4C3, 4E5, GBO4, ECO2 and ECO1 recognize the N-terminal epitope of the NP. The MAbs F23A1 and E5/G6 recognize aa 291–402 and aa 165–173 of the NP, respectively (Lundkvist et al., 1991; Ruo et al., 1991; Yoshimatsu et al., 1996). The epitope for MAb C16D11 is unknown. MAbs except for GBO4 and ECO1 were obtained from the cell culture supernatant. The MAbs GBO4 and ECO1 were obtained from ascitic fluid. Sera from three patients infected with SNV were supplied kindly by Brian Hjelle of the University of New Mexico Health Sciences Center, New Mexico, USA. Negative control human sera were obtained from healthy volunteers. This study was approved by the ethics committee of Hokkaido University Graduate School of Medicine, and informed consent was obtained from all human subjects, including healthy volunteers. Three sera from *Peromyscus maniculatus* infected with SNV and one serum from hantavirus-uninfected *P. maniculatus* were supplied kindly by David Safronetz of the National Institute of Allergy and Infectious Diseases, National Institutes of Health, Montana, USA. Several species of *Reithrodontomys* were captured in Guerrero, Mexico. Three *R. sumichrasti* were infected with CARV, and one *R. megalotis* was infected with Huitzilac virus (HUIV), which showed 96.7% amino acid identity to NP of CARV (Kariwa et al., 2012). Sera from hantavirus-uninfected *P. maniculatus*, *R. sumichrasti* and *R. megalotis* were used as negative controls. These viral types in the patients and rodents were determined by detection of the virus genome by reverse transcriptase (RT)-PCR.

2.3. Amino acid and nucleotide sequence comparison and phylogenetic analysis

Amino acid and nucleotide sequences of the variable region in NP (230–302 aa and 690–906 nucleotides) of New World hantavirus in North America and South America were aligned and compared with sequences determined previously using GenetyxMac Ver.13 (Genetyx Corporation, Tokyo, Japan). Phylogenetic relationships among the hantavirus sequences of the variable region of NP were evaluated using the Neighbor-Joining program with the Kimura 2 parameter distance in CLUSTALW version 1.83 (European Bioinformatics Institute, Cambridge, UK). The phylogenetic tree was visualized using the NJ plot program (Perriere and Gouy, 1996). Bootstrap resampling analysis was performed using 1000 replicates.

2.4. Construction of recombinant baculoviruses expressing whole rNPs and trNPs

The gene encoding whole NP (aa 1–428) and truncated genes encoding truncated NP (aa 50–428 and aa 100–428) were PCR-amplified from cDNA of the S segment. The primers listed below were used for amplification of whole and truncated S segments. A 5′ SpeI site and a 3′ XhoI site were introduced into the primers (both sites shown in italics). Primer sequences (forward and reverse) were as follows: SNV whole rNP, 5′-gac*actagt*atgagcaccctcaaagaa-3′ and 5′-tac*ctcgag*ttaaagtttaagtttaagtggttc-3′; CARV whole rNP, 5′-aaa*actagt*atgagcaacctcaaagaa-3′ and 5′-gat*ctcgag*ttatagttttagagg-3′; BCCV whole rNP, 5′-gaa*actagt*atgagcaacctcaaagaa-3′ and 5′-gatt*ctcgag*tcatatctttaaaggctc-3′; SNV trNP50, 5′-tcg*actagt***atg**gctgtgtctgcattggag-3′ and 5′-tac*ctcgag*ttaaagtttaagtttaagtggttc-3′; CARV trNP50, 5′-aga*actagt***atg**gctgtgtctgcattggaa-3′ and 5′-gat*ctcgag*ttatagttttagagg-3′; BCCV trNP50, 5′-aac*actagt***atg**gctgtgtctgcattggag-3′ and 5′-gatt*ctcgag*tcatatctttaaaggctc-3′; SNV trNP100, 5′-tcg*actagt***atg**gctgtgtctgcattggag-3′ and 5′-tac*ctcgag*ttaaagtttaagtttaagtggttc-3′; CARV trNP100, 5′-aga*actagt***atg**gctgtgtctgcattggaa-3′ and 5′-gat*ctcgag*ttatagttttagagg-3′; BCCV trNP100, 5′-ctt*actagt***atg**aatgtgcttgacgtcaat-3′ and 5′-gatt*ctcgag*tcatatctttaaaggctc-3′. Boldface indicates an added start codon. After amplification, the DNA fractions were subcloned into pFastBac1 (Invitrogen, Groningen, The Netherlands). The recombinant baculoviruses were expressed using the Bac-to-Bac Baculovirus Expression System (Invitrogen) according to the manufacturer's instructions. Mock baculovirus was made from original pFastBac1. The titers of recombinant baculoviruses in the culture supernatant were determined by 50% tissue culture infective dose ($TCID_{50}$) with High Five cells.

2.5. Preparation of whole rNPs and trNPs expressed by baculoviruses

High Five cells (Invitrogen) were grown in Grace's insect cell culture medium (Invitrogen) supplemented with 10% fetal bovine serum as described previously (Araki et al., 2001). High Five cells were infected with recombinant baculoviruses at a multiplicity of infection of 1 for 3 days. Collection and lysis of infected cells were performed using methods described previously (Araki et al., 2001). Briefly, infected High Five cells were collected in phosphate-buffered saline (PBS) of 2.5×10^6 cells/mL and sonicated. The cell lysate containing recombinant NP (rNP) was used as ELISA antigen. The lysate of cells infected with mock baculovirus was used as a negative control. The expression of rNPs of SNV, CARV and BCCV was confirmed by Western blotting (data not shown) using methods described previously (Yoshimatsu et al., 1995). High Five cells expressing whole recombinant NPs (whole rNPs) of PUUV

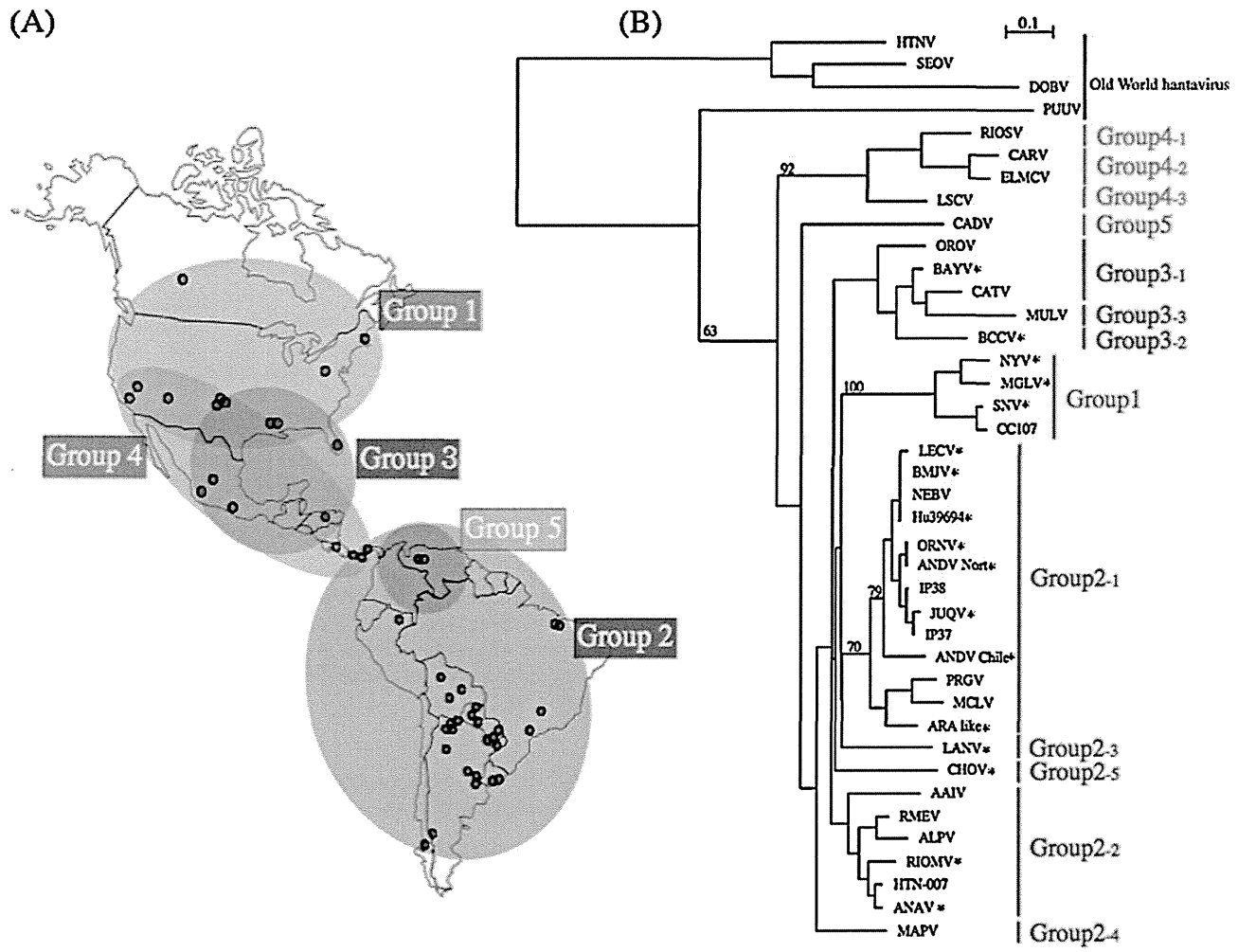

Fig. 1. Distribution map of grouped New World hantaviruses and phylogenetic tree for New World hantavirus. (A) The map represents the geographical distribution of grouped New World hantaviruses. (B) Phylogenetic tree for New World hantavirus. Neighbor-joining phylogenetic analysis was performed on the basis of partial aa sequences of S (aa 230–302). An asterisk (*) indicates that human cases of infection with the virus have been reported. Abbreviations: AAIV, Ape Aime Itapua virus, Hantavirus strain IP16 (GenBank ID: DQ345764); ALPV, Alto Paraguay virus (GenBank ID: DQ345762); ANAV, Anajatuba virus (GenBank ID: DQ451829); ANDV Chile, Andes virus Chile-9717869 (GenBank ID: AF291702); ANDV Nort, Andes virus AND Nort (GenBank ID: AF325966); ARA like, Araraquara-like virus strain P5/Cajuru (GenBank ID: EF571895); BAYV, Bayou virus (GenBank ID: L36929); BCCV, Black Creek Canal virus (GenBank ID: L39949); BMJV, Bermejo virus (GenBank ID: AF482713); CARV, Carrizal virus (GenBank ID: AB620093); CATV, Catacamas virus (GenBank ID: DQ256126); CC107, Convict Creek 107 virus (GenBank ID: L33683); CADV, Cano Delgadito virus (GenBank ID: DQ285566); CHOV, Choclo virus (GenBank ID: DQ285046); DOBV, Dobrava-Belgrade virus (GenBank ID: L41916); ELMCV, El Moro Canyon virus (GenBank ID: U11427); HTNV, Hantaan virus (GenBank ID: M14626); HTN-007, Hantavirus HTN-007 (GenBank ID: AF133254); Hu39694, Hu39694, Hantavirus sp. (GenBank ID: AF482711); IP37, Hantavirus strain Itapua 37 (GenBank ID: DQ345765); IP38, Hantavirus strain Itapua 38 (GenBank ID: DQ345766); JUQV, Juquitiba virus (GenBank ID: EF492472); LANV, Laguna Negra virus (GenBank ID: AF005727); LECV, Lechiguanas virus (GenBank ID: AF482714); LSCV, Limestone Canyon virus (GenBank ID: AF307322); MCLV, Maciel virus (GenBank ID: AF482716); MAPV, Maporal virus (GenBank ID: AY267347); MGLV, Hantavirus Monongahela-1 (GenBank ID: U32591); MULV, Muleshoe virus (GenBank ID: U54575); NEBV, Neembucu hantavirus (GenBank ID: DQ345763); NYV, New York virus (GenBank ID: U09488); ORNV, Oran virus (GenBank ID: AF482715); OROV, Playa de Oro hantavirus (GenBank ID: EF534079); PRGV, Pergamino virus (GenBank ID: AF482717); PUUV, Puumala virus (GenBank ID: X61035); RIOMV, Rio Mamore virus (GenBank ID: U52136); RMEV, Rio Mearim virus (GenBank ID: DQ451828); RIOSV, Rio Segundo virus (GenBank ID: U18100); SEOV, Seoul, Sapporo rat virus (GenBank ID: M34881); SNV, Sin Nombre virus SN 77734 (GenBank ID: AF281851).

and HTNV were prepared as described previously (Araki et al., 2001). High Five cells expressing whole rNPs and trNPs were used for IFA.

2.6. Preparation of rNPs expressed by Escherichia coli

Whole rNPs of SNV, CARV and BCCV fused with a Nus-tag and His-tag were expressed in *E. coli*. DNA fractions containing the entire coding region of NP of SNV, CARV and BCCV were made by digestion of pFastBac1 including the cDNA with SalI and XhoI. The DNA fractions were subcloned into the pET43b vector (Merck KGaA, Darmstadt, Germany) and transfected into *E. coli* strain BL21 (DE3) (Merck KGaA). A single colony was inoculated into Circle growth medium (MP Biomedicals, Morgan Irvine, CA, USA) containing ampicillin (50 μg/mL) for small-scale culture incubation at 37 °C overnight. After the culture fluid had been centrifuged, the collected cells were inoculated into 100 mL of Circle growth medium, and Isopropyl β-D-1-thiogalactopyranoside (IPTG) induction was performed according to the procedure for pET system expression. The cultured cells were collected by centrifugation, resuspended in 5 mL of 0.5 M NaCl binding buffer (0.5 M NaCl, 20 mM imidazole, 20 mM potassium phosphate), and sonicated four times for 15 s each time on ice. Thereafter, the fusion protein was purified using a His-Trap HP (GE Healthcare, Buckinghamshire, UK) according to the manufacturer's instructions. An antigen made from the original pET43b vector was used as a negative control. The purities of recombinant antigen were confirmed by sodium dodecyl sulfate-polyacrylamide gel electrophoresis (SDS-PAGE) (data not shown).

2.7. IFA test

Acetone-fixed smears of High Five cells infected with recombinant baculoviruses were used as antigens. The detailed procedure was described previously (Morii et al., 1998; Yoshimatsu et al., 1993). MAbs obtained from the cell culture supernatant were used without dilution. MAbs GBO4 and ECO1 obtained from ascitic fluid were used at 100-fold dilution.

2.8. Detection of multimerized rNPs

To detect multimerization of the rNPs expressed by the baculovirus, competitive-sandwich ELISA was performed with MAb E5/G6 recognizing aa 165–173 as a capture and detector antibody. Briefly, rNPs were captured on the plate with MAb E5/G6 followed by detection with the same MAb E5/G6. Positive reaction with this ELISA indicates that the antigens are forming a multimer (Yoshimatsu et al., 2003).

2.9. ELISA with whole rNPs expressed by E. coli

ELISA using whole rNPs expressed by *E. coli* was carried out as described previously (Koma et al., 2010). Patient and rodent sera were used at 200-fold dilution. Horseradish peroxidase (HRP)-labeled goat anti-human IgG (H + L) antibody (KPL, Gaithersburg, MD, USA) for patient sera and HRP-labeled goat anti-*Peromyscus leucopus* IgG (H + L) antibody (KPL) for *Peromyscus* and *Reithrodontomys* sera were used as secondary antibodies. Color reactions were performed with *o*-phenylenediamine dihydrochloride (OPD) (Sigma–Aldrich, St. Louis, MO) and allowed to develop for 10–15 min. Absorbance was measured at 450 nm by using a SpectraMax 340 microplate spectrophotometer (Molecular Device, Sunnyvale, CA). An antigen made from the original pET43b vector was used as a negative control.

2.10. Serotyping ELISA with trNPs expressed by baculovirus

The serotyping ELISA was performed as described previously (Koma et al., 2010; Nakamura et al., 2008). Ninety-six-well plates were coated with MAb E5/G6 (2 μg/mL in PBS) as a capture antibody. Patient and rodent sera were used at 200-fold dilution. HRP-labeled goat anti-human IgG (H + L) antibody (KPL) for patient sera and HRP-labeled goat anti-*Peromyscus leucopus* IgG (H + L) antibody (KPL) for *Peromyscus* and *Reithrodontomys* sera were used as secondary antibodies. Color development results were the same as those for the ELISA with whole rNPs. Cell lysate infected with mock baculovirus was used as a negative control.

3. Results

3.1. Grouping of New World hantaviruses by comparison of the variable region of NP

New World hantaviruses were divided into five groups (groups 1–5) based on the identity of aa in the internal variable region (aa 230–302) (Table 1). Groups were defined as more than approximately 70% amino acid sequence identity except for Bayou virus (BAYV) and Playa de Oro virus (OROV) in group 3. These two hantaviruses have more than 70% amino acid sequence identity to those of most of the viruses in group 2, but they have higher amino acid sequence identity to those of viruses in group 3. Subgroups were defined as more than approximately 80% of amino acid identity. Based on this classification, groups 2, 3 and 4 were divided into five, three and three subgroups, respectively. This classification corresponded to geographical characteristics and clades of the phylogenetic tree of the virus (Fig. 1). The endemic areas of groups 1, 3 and 4 were overlapped in the southern area of the United States. In this study, SNV, BCCV and CARV were selected as representative viruses of groups 1, 3 and 4, respectively. As shown in Table 1, aa sequence identities among SNV, BCCV and CARV ranged from 49.3% to 54.8%.

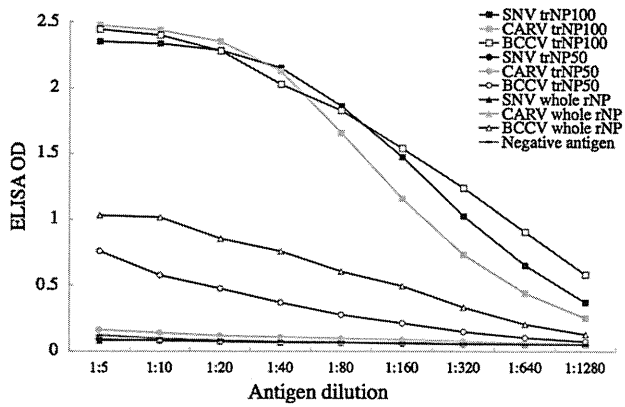

Fig. 2. Multimerization of rNPs in competitive-sandwich ELISA. Antigens were captured and detected with MAb E5/G6. Each antigen was diluted from 1:5 to 1:1280 and subjected to capture ELISA. Positive reaction with this ELISA indicates that the antigens are forming a multimer. The ELISA was performed three times and the representative OD value was plotted.

3.2. Antigenic characterization of rNPs expressed by recombinant baculovirus with MAbs in IFA tests

Antigenic profiling of whole rNPs or trNPs of SNV, CARV and BCCV expressed in High Five cells was carried out using hantavirus-specific MAbs (Table 2). Whole rNPs of SNV, CARV and BCCV reacted to cross-reactive MAbs (2E12, 4C3, 4E5, GBO4, C16D11, ECO2 and ECO1) that recognized immunodominant epitopes of the N-terminus of NP, except for C16D11, and cross-reactive MAbs (F23A1 and E5/G6) that recognized the C-terminus of NP aa 291–402 and aa 166–175, respectively. The reactivity pattern of the SNV whole rNP was different from those of the whole rNPs of CARV and BCCV with MAbs C16D11 and ECO2. The trNP50s of SNV, CARV and BCCV lacked reactivity with 5 of the N-terminal specific MAbs (2E12, 4C3, 4E5, ECO2 and ECO1) but still reacted with MAb GBO4, which recognized the N-terminus. The trNP100s reacted to only two cross-reactive MAbs, E5/G6 and F23A1.

3.3. Detection of multimerization of rNPs

Multimerization activities of whole rNPs, trNP50s and trNP100s were compared among those from SNV, CARV and BCCV. As shown in Fig. 2, there was no reaction to trNP50s and whole rNPs of SNV and CARV. This implied that the trNP50s and whole rNPs captured by E5/G6 could not react with E5/G6 as a detector due to competition. Thus, trNP50s and whole rNPs of SNV and CARV were considered as monomers. On the other hand, there were strong reactions to trNP100s, indicating that trNP100s of SNV, CARV and BCCV existed as multimers. There were moderate reactions to whole rNP and trNP50 of BCCV. Since serotype-specific epitopes have been suggested to be formed after multimerization of trNPs (Yoshimatsu et al., 2003), trNP100s were selected as ELISA antigens for serotyping ELISA. The reactivities of trNP100s of SNV, CARV and BCCV were nearly equivalent at antigen dilutions of 1:5 to 1:40. Therefore, the antigens were used at 10-fold dilution.

Table 1
Identity of amino acid (upper right) and nucleotide (lower left) sequences of the S segment of hantaviruses.

	Group 1			Group 2-1								2-2				2-3	2-4	2-5	Group 3-1			3-2	3-3	Group 4-1	4-2		4-3	Group 5	Old World hantavirus			
				Hu				AND	ARA																						
Virus	SN	NY	MGL	39694	LEC	ORN	JUQ	Chile	like	PRG	MCL	ANA	RIOM	ALP	AAI	LAN	MAP	CHO	BAY	ORO	CAT	BCC	MUL	RIOS	ELMC	CAR	LSC	CAD	PUU	HTN	SEO	DOB
SN		**84.9**	**78.1**	**69.9**	**68.5**	**67.1**	**67.1**	**61.6**	**67.1**	**63.0**	**61.6**	**64.4**	**61.6**	**64.4**	**65.8**	**63.0**	**60.3**	**61.6**	**60.3**	**61.6**	**60.3**	**53.4**	**52.1**	**57.5**	**56.2**	**54.8**	**54.8**	**57.5**	**39.7**	**28.8**	**26.0**	**23.3**
NY	82.6		89.0	65.8	64.4	63.0	63.0	61.6	64.6	63.0	60.3	65.8	63.0	64.4	65.8	64.4	60.3	61.6	61.6	63.0	63.0	**56.2**	56.2	53.4	53.4	**52.1**	54.8	56.2	35.6	30.1	26.0	24.7
MGL	74.9	82.2		68.5	67.1	65.8	63.0	64.4	64.4	64.4	61.6	64.6	61.6	63.0	67.1	63.0	60.3	61.6	61.6	60.3	61.6	**67.5**	53.4	49.3	49.3	**47.9**	52.1	54.8	37.0	28.8	26.0	24.7
Hu39694	65.3	63.5	68.8		98.6	95.9	91.8	89.0	86.3	82.2	80.8	76.7	76.7	74.0	72.6	74.0	72.6	71.2	74.0	72.6	65.8	**68.5**	60.3	50.7	49.3	**49.3**	56.2	63.0	41.1	32.9	27.4	27.4
LEC	68.5	63.5	66.4	81.3		94.5	90.4	87.7	84.9	80.8	79.5	75.3	78.1	72.6	71.2	72.6	74.0	69.9	72.6	71.2	64.4	**67.1**	58.9	52.1	47.9	**47.9**	54.8	64.4	39.7	34.2	28.8	28.8
ORN	68.0	67.0	68.7	80.4	85.4		94.5	86.3	83.6	80.8	79.5	75.3	75.3	72.6	71.2	72.6	71.2	68.5	72.6	71.2	64.4	**67.1**	58.9	50.7	49.3	**49.3**	56.2	60.3	39.7	32.9	27.4	29.2
JUQ	67.6	66.7	64.2	78.1	78.5	78.1		87.7	82.2	78.1	79.5	78.1	74.0	71.2	69.9	75.3	71.2	71.2	71.2	72.6	65.8	**64.4**	57.5	50.7	50.7	**49.3**	57.5	60.3	39.7	31.5	28.8	27.4
AND Chile	64.8	68.3	66.5	75.8	76.3	74.4	73.5		79.5	80.8	78.1	75.3	72.6	67.1	68.5	71.2	72.6	69.9	71.2	68.5	64.4	**67.1**	61.6	49.3	46.6	**45.2**	58.9	60.3	39.7	30.1	30.1	28.8
ARA like	70.3	63.0	64.8	76.7	77.2	75.8	70.3	73.1		84.9	83.6	78.1	72.6	78.1	71.2	71.2	74.0	71.2	74.0	74.0	68.5	**64.4**	65.8	52.1	53.4	**53.4**	56.2	60.3	43.8	32.9	27.4	28.8
PRG	67.1	66.7	68.8	74.9	74.4	74.4	74.4	73.5	76.7		89.0	76.7	74.0	75.3	67.1	69.9	72.6	68.5	71.2	74.0	65.8	**65.8**	61.6	52.1	49.3	**50.7**	61.6	56.2	43.8	28.8	27.4	30.5
MCL	65.6	63.3	61.5	73.5	78.1	77.2	73.1	73.5	74.4	77.2		76.7	74.0	76.7	68.5	65.8	71.2	65.8	69.9	72.6	65.8	**65.8**	61.6	52.1	52.1	**49.3**	61.6	56.2	46.6	28.8	28.8	27.4
ANA	67.6	63.0	61.6	71.2	74.0	71.7	73.1	67.1	72.1	68.0	68.5		90.4	89.0	78.1	78.1	79.5	75.3	72.6	74.0	71.2	**67.1**	61.6	54.8	52.1	**53.4**	64.4	61.6	38.4	32.9	30.1	26.0
RIOM	64.8	67.9	66.1	68.9	73.1	71.7	69.9	68.0	69.9	70.3	66.2	81.7		82.2	78.1	75.3	78.1	69.9	69.9	69.9	67.1	**67.1**	58.9	56.2	50.7	**52.1**	63.0	60.3	37.0	35.6	34.2	27.4
ALP	66.2	66.5	67.4	70.3	70.8	70.3	67.1	64.8	69.9	68.9	67.6	78.5	74.4		78.1	74.0	71.2	65.8	69.9	68.5	67.1	**65.8**	60.3	56.2	56.2	**56.2**	60.3	64.4	41.1	28.8	27.4	26.0
AAI	67.6	66.2	63.0	68.0	66.7	68.0	70.8	64.4	66.7	69.9	68.0	72.6	72.6	73.1		68.5	71.2	68.5	74.0	71.2	68.5	**65.8**	61.6	54.8	52.1	**52.1**	57.5	60.3	35.6	32.9	27.4	24.7
LAN	62.6	63.9	63.8	71.7	66.7	68.9	74.4	68.9	68.9	69.9	63.0	71.2	74.9	67.6	67.6		71.2	67.1	64.4	68.5	64.4	**60.3**	54.8	54.8	54.8	**56.2**	56.2	60.3	35.6	34.2	27.4	26.0
MAP	63.0	62.6	63.6	67.1	68.0	67.1	67.6	67.1	67.1	69.4	67.1	70.3	74.9	68.0	72.1	68.5		68.5	74.0	69.9	69.9	**65.8**	61.6	56.2	50.7	**52.1**	61.6	61.6	37.0	38.4	34.2	32.9
CHO	60.3	58.9	61.0	69.4	66.7	65.3	65.8	66.2	65.3	66.2	66.7	68.0	65.8	64.8	66.2	66.2	63.0		69.9	67.1	64.4	**63.0**	58.9	53.4	53.4	**53.4**	60.3	58.9	38.4	30.1	27.4	26.0
BAY	63.9	66.7	60.7	63.5	66.2	67.1	67.6	63.5	68.0	66.2	63.5	68.9	68.5	65.8	70.8	66.7	67.1	64.2		86.3	87.7	**82.2**	80.8	58.9	57.5	**54.8**	60.3	54.8	39.7	31.5	27.4	27.4
ORO	63.9	62.6	61.6	69.9	68.9	68.5	71.2	63.9	68.5	69.4	65.3	69.4	68.0	65.8	70.8	68.9	68.0	66.7	75.8		82.2	**72.6**	74.0	58.9	54.8	**53.4**	58.9	53.4	41.1	30.1	27.4	31.5
CAT	62.1	61.2	59.4	61.6	64.4	63.0	65.8	64.8	64.8	66.7	62.6	65.8	65.8	66.7	67.6	66.2	67.1	63.9	78.5	76.3		**74.0**	78.1	58.9	56.2	**53.4**	56.2	52.1	39.7	32.9	26.0	27.4
BCC	63.3	62.4	61.0	63.5	68.9	65.3	68.5	64.8	65.3	66.2	64.8	68.9	69.9	68.9	67.1	66.7	68.9	66.7	75.3	74.0	75.8		**71.2**	**53.4**	**50.7**	**49.3**	**57.5**	**52.1**	**46.6**	**30.1**	**28.8**	**27.4**
MUL	62.1	60.3	58.9	62.6	65.4	65.0	65.1	64.1	61.6	67.3	64.7	67.6	64.4	65.1	66.2	65.1	65.8	62.6	73.5	70.8	74.4	76.1		50.7	49.3	**46.6**	52.1	49.3	43.8	27.8	24.7	27.4
RIOS	60.3	57.5	57.1	61.6	60.6	63.3	61.2	60.3	61.2	62.4	58.3	59.4	61.6	63.0	61.6	60.3	63.0	63.9	62.1	64.4	61.5	61.5	60.6		78.1	**78.1**	69.9	53.4	34.2	28.8	27.4	28.8
ELMC	58.4	56.6	60.4	58.4	58.0	60.6	60.3	63.1	62.8	60.1	58.0	59.2	59.2	58.7	59.8	57.3	61.6	57.8	59.8	63.5	62.8	63.0	56.2	74.0		**90.4**	74.0	54.8	32.9	27.4	27.4	26.0
CAR	64.4	61.1	59.9	56.2	58.0	61.3	57.1	54.8	58.7	59.2	63.1	61.5	58.5	61.8	63.1	60.4	57.1	63.1	61.2	61.5	60.4	61.0	62.7	68.5	74.9		**69.9**	**53.4**	**32.9**	**30.1**	**23.3**	**26.0**
LSC	61.2	56.6	55.3	62.6	62.8	63.8	60.3	60.3	63.0	62.1	61.6	64.2	63.3	61.6	64.8	55.7	63.0	61.6	59.4	65.8	58.4	64.4	60.3	68.9	71.7	68.0		52.1	34.2	30.1	32.9	28.8
CAD	63.6	63.3	58.9	66.1	71.4	66.1	71.9	65.6	65.6	64.2	64.8	66.5	60.7	65.6	64.8	64.2	67.0	61.9	65.1	60.3	58.9	61.9	59.8	65.0	66.4	62.4	63.1		35.6	31.5	24.7	26.0
PUU	53.9	54.4	56.0	56.4	53.0	58.7	61.8	58.0	53.9	59.2	58.1	51.6	53.7	57.8	56.6	59.3	56.9	54.8	53.9	55.8	56.6	56.7	54.2	55.0	57.1	60.5	51.1	51.9		24.3	27.0	28.4
HNT	55.2	54.6	52.1	53.7	52.6	50.9	61.6	54.2	52.8	55.6	52.3	53.5	60.3	48.4	52.3	56.9	55.9	53.2	53.2	53.5	53.2	55.4	56.9	51.9	50.2	48.4	56.9	55.7	53.3		54.1	58.1
SEO	47.5	52.9	48.2	55.3	56.5	54.9	48.2	53.5	50.2	53.3	45.0	48.4	47.0	50.7	46.5	49.7	53.7	47.5	47.2	48.1	51.0	50.9	47.5	54.9	52.1	50.6	47.5	49.1	47.9	61.2		56.8
DOB	53.5	50.0	53.8	52.1	54.0	52.7	51.5	51.2	49.8	51.2	49.8	53.7	53.5	52.9	51.6	55.0	53.1	54.7	50.7	56.1	46.5	50.9	48.8	46.8	51.6	54.9	54.9	51.9	53.4	59.5	64.3	

Amino acid and nucleotide identities of variable region (230–302 amino acids and 690–906 nucleotides). Abbreviations: AAI, Ape Aime Itapua virus, Hantavirus strain IP16 (GenBank ID: DQ345764); ALP, Alto Paraguay virus (GenBank ID: DQ345762); ANA, Anajatuba virus (GenBank ID: DQ451829); AND Chile, Andes virus Chile-9717869 (GenBank ID: AF291702); ARA like, Araraquara-like virus strain P5/Cajuru (GenBank ID: EF571895); BAY, Bayou virus (GenBank ID: L36929); BCC, Black Creek Canal virus (GenBank ID: L39949); CAR, Carrizal virus (GenBank ID: AB620093); CAT, Catacamas virus (GenBank ID: DQ256126); CAD, Cano Delgadito virus (GenBank ID: DQ285566); CHO, Choclo virus (GenBank ID: DQ285046); DOB, Dobrava-Belgrade virus (GenBank ID: L41916); ELMC, El Moro Canyon virus (GenBank ID: U11427); HTN, Hantaan virus (GenBank ID: M14626); Hu39694, Hu39694, Hantavirus sp. (GenBank ID: AF482711); JUQ, Juquitiba virus (GenBank ID: EF492472); LEC, Lechiguanas virus (GenBank ID: AF482714); LAN, Laguna Negra virus (GenBank ID: AF005727); LSC, Limestone Canyon virus (GenBank ID: AF307322); MCL, Maciel virus (GenBank ID: AF482716); MAP, Maporal virus (GenBank ID: AY267347); MGL, Hantavirus Monongahela-1 (GenBank ID: U32591); MUL, Muleshoe virus (GenBank ID: U54575); NY, New York virus (GenBank ID: U09488); ORN, Oran virus (GenBank ID: AF482715); ORO, Playa de Oro hantavirus (GenBank ID: EF534079); PRG, Pergamino virus (GenBank ID: AF482717); PUU, Puumala virus (GenBank ID: X61035); RIOM, Rio Mamore virus (GenBank ID: U52136); RIOS, Rio Segundo virus (GenBank ID: U18100); SEO, Seoul, Sapporo rat virus (GenBank ID: M34881); SN, Sin Nombre virus SN 77734 (GenBank ID: AF281851).

Table 2
Antigenic characterization of rNPs expressed by recombinant baculovirus with MAbs in the IFA test.

Origin	MAbs	Epitope	Whole rNP						trNP50			trNP100		
			PUUV[a]	HTNV[a]	SEOV[a]	SNV[a]	CARV[a]	BCCV[a]	SNV	CARV	BCCV	SNV	CARV	BCCV
PUUV	2E12	N-terminus	+[b]	±	±	+	+	+	–	–	–	–	–	–
	4C3	N-terminus	+	+	+	+	+	+	–	–	–	–	–	–
	4E5	N-terminus	+	+	±	+	+	+	–	–	–	–	–	–
	GBO4[c]	N-terminus	+	+	+	+	+	+	±	+	±	–	–	–
HTNV	C16D11	Unknown	+	+	+	–	+	+	–	+	+	–	–	–
	ECO2	aa 1–33	–	+	+	–	+	+	–	–	–	–	–	–
	ECO1[c]	aa 34–103	+	+	+	+	+	+	–	–	–	–	–	–
	F23A1	aa 291–402	–	+	+	+	+	+	+	±	+	+	±	+
	E5/G6	aa 165–173	+	+	+	+	+	+	+	+	+	+	+	+

[a] PUUV, Puumala virus; HTNV, Hantaan virus; SEOV, Seoul virus; SNV, Sin Nombre virus; CARV, Carrizal virus; BCCV, Black Creek Canal virus.
[b] Symbols: +, positive IFA result of >1:1 (1:100 for ascitic fluid samples); ±, scarcely positive IFA result; –, negative IFA result.
[c] The sample was ascitic fluid.

3.4. Reactivities of whole rNP and trNP100s with infected patient and rodent sera

Applicability of the trNP100s in ELISA was examined using patient and rodent sera. As shown in Fig. 3A, whole rNPs of SNV, CARV and BCCV expressed by *E. coli* showed strong cross-reactivity, but trNP100s of SNV and CARV expressed by baculoviruses showed strong reactions to homologous antigen and weak reactions to heterologous antigen (Fig. 3B). The ELISA ODs for the homologous reaction were more than twice those for the heterologous reactions. There was no serum from a BCCV-infected patient or rodent, but the trNP100 of BCCV also showed weak reactivity to heterologous sera.

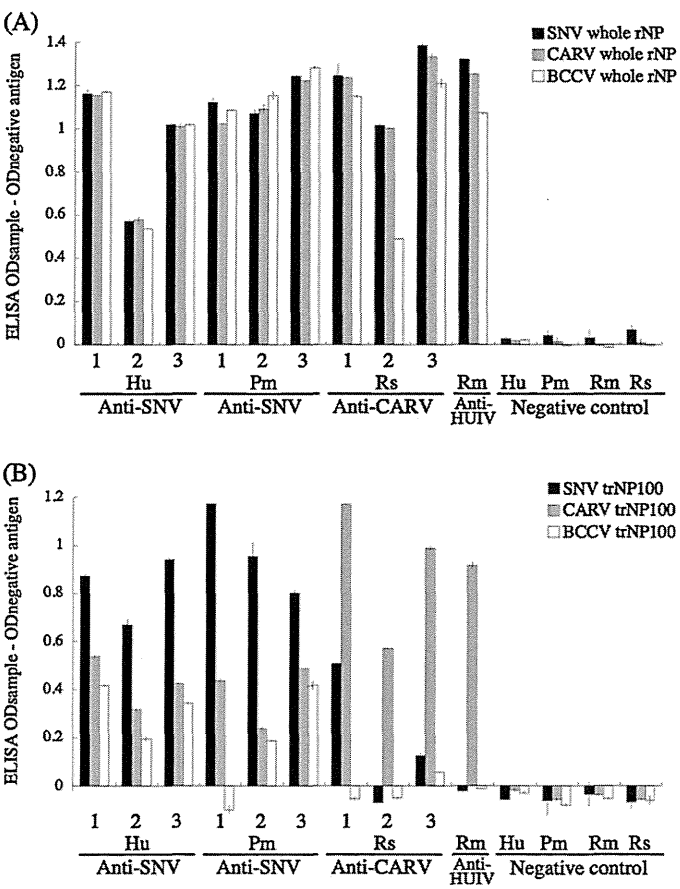

Fig. 3. Reaction patterns of hantavirus-positive and -negative sera in ELISA. (A) Reaction patterns of whole rNPs (SNV, CARV and BCCV) with human and rodent sera in ELISA. (B) Reaction patterns of trNP100s (SNV, CARV and BCCV) with human and rodent sera in ELISA. Abbreviations: Hu, human serum; Pm, *Peromyscus maniculatus* serum; Rs, *Reithrodontomys sumichrasti* serum; Rm, *Reithrodontomys megalotis* serum; Anti-SNV, serum from patients with HPS or *P. maniculatus* infected with Sin Nombre virus; Anti-CARV, serum from Carrizal virus-infected *R. sumichrasti*; Anti-HUIV, serum from Huitzilac virus-infected *R. megalotis*. The OD value was corrected by subtracting the OD value with negative control antigen. The ELISA was performed three times in duplicate and the bar shows the mean values of a representative experiment.

4. Discussion

New World hantaviruses were divided into five groups and groups 2, 3 and 4 were further divided into five, three and three subgroups, respectively, by comparison of amino acid sequence identity (aa 230–302) of the variable region of NP (Table 1). These hantaviruses were also grouped into five corresponding groups geographically and phylogenetically (Fig. 1A and B). This classification corresponds basically to a previous study in which hantaviruses were classified by comparison of the entire amino acid sequences of S and M segments (Maes et al., 2009).

As shown in Fig. 1B, groups 1, 2 and 3 include hantaviruses that are pathogenic to humans. On the other hand, hantaviruses in groups 4 and 5 have not been reported to cause disease in humans. Thus, serotyping among infections is important for clinical diagnosis and epidemiological surveillance in regions where two or more hantaviruses co-circulate.

In this study, the applicability of N-terminally truncated rNPs of those three hantavirus species as antigens for serotyping ELISA to differentiate SNV and CARV infection was investigated. Sera from SNV- and CARV-infected rodents or humans reacted strongly to homologous antigens. In contrast, these sera reacted weakly to heterologous antigens including BCCV trNP100 (Fig. 3). The trNP100s of SNV, CARV and BCCV could distinguish human and rodent sera. Together with the work reported previously (Koma et al., 2010), trNP100s of SNV (group 1), ANDV (group 2), BCCV (group 3) and CARV (group 4) have been prepared. They can distinguish infections between groups except for group 5 in the New World hantaviruses. On the other hand, the whole rNPs of SNV, BCCV and CARV expressed by *E. coli* reacted strongly at almost equal levels to all of the heterologous sera. Therefore, screening ELISA using whole rNPs from any one of the New World hantaviruses followed by serotyping ELISA using the trNPs is recommended as a rapid and practical system for hantavirus seroepidemiology.

There have been few reports on MAbs to NP of New World hantaviruses (Tischler et al., 2008). Consequently, antigenic characterization of rNPs was indirectly confirmed using MAbs to Old World hantaviruses by IFA. MAbs that recognize immunodominant epitopes of the N-terminus of NP reacted to whole rNPs and trNP50s but not to trNP100s in IFA (Table 2). These results support those of previous studies indicating that the first 100 aa of the N-terminus of NP possess immunodominant, cross-reactive epitopes (Elgh et al.,

1996; Gott et al., 1997; Vapalahti et al., 1995; Yamada et al., 1995) and suggest that these cross-reactive epitopes are conserved highly among both the New World and the Old World hantaviruses. Only MAb E5/G6 that bound to the conserved linear epitope recognized commonly all rNPs (Okumura et al., 2004). Thus, MAb E5/G6 could be used as a capture antibody for both the rNPs of New World and Old World hantaviruses and also as a detection antibody.

It has been reported that conformation-dependent, serotype-specific epitopes in NP are located from aa 205 to 290 (Yoshimatsu et al., 1996, 2003). The major linear epitopes in NP have been reported to be located at the N-terminus (Elgh et al., 1996; Gott et al., 1997; Yamada et al., 1995). Therefore, truncated rNPs that lacked only a minimal region were applied and trNP50s were prepared as well as trNP50s for Old World hantaviruses that were reported previously (Araki et al., 2001). However, trNP50s of SNV and CARV were found as monomeric NP in the competitive-sandwich ELISA (Fig. 2). Furthermore, the trNP50s showed higher cross-reactivity with each other (data not shown). Therefore, trNP50s of those were not applicable for serotyping antigens. The results indicated that trNP50s still possessed cross-reactivity to heterologous sera. In contrast, trNP100s of SNV, CARV and BCCV were detected as multimers (Fig. 2). The whole rNP and trNP50 of BCCV reacted to detector MAb E5/G6 in the competitive-sandwich ELISA, but the reaction was weak in comparison to reaction of the BCCV trNP100. These results support results of other studies indicating that the first 100 aa of the N-terminus did not contribute to NP-NP interaction (Kaukinen et al., 2004; Yoshimatsu et al., 2003).

In terms of public health, it is important to develop rapid, safe and convenient serotyping methods for epidemiological surveillance and studies. This system will become a valuable tool for surveying human and rodent cases of New World hantavirus infections.

Acknowledgements

This work was supported by the Global COE Program "Establishment of an International Collaboration Center for Zoonosis Control" from the Japanese Ministry of Education, Culture, Sports, Science and Technology, Japan. This work was supported also partially by Grants-in-Aid for Scientific Research and the Development of Scientific Research from the Japanese Ministry of Health, Labour and Welfare, Japan (200829018A). This study was supported in part by the Program of Founding Research Centers for Emerging and Reemerging Infectious Diseases, MEXT, Japan. We would like also to acknowledge Stewart Chisholm of the Stewart English School (S.E.S.) for revising the grammar in the final manuscript.

References

Araki, K., Yoshimatsu, K., Ogino, M., Ebihara, H., Lundkvist, A., Kariwa, H., Takashima, I., Arikawa, J., 2001. Truncated hantavirus nucleocapsid proteins for serotyping Hantaan, Seoul, and Dobrava hantavirus infections. Journal of Clinical Microbiology 39, 2397–2404.

Botten, J., Mirowsky, K., Kusewitt, D., Bharadwaj, M., Yee, J., Ricci, R., Feddersen, R.M., Hjelle, B., 2000. Experimental infection model for Sin Nombre hantavirus in the deer mouse (*Peromyscus maniculatus*). Proceedings of the National Academy of Sciences of the United States of America 97, 10578–10583.

Elgh, F., Lundkvist, A., Alexeyev, O.A., Wadell, G., Juto, P., 1996. A major antigenic domain for the human humoral response to Puumala virus nucleocapsid protein is located at the amino-terminus. Journal of Virological Methods 59, 161–172.

Elliott, R.M., 1990. Molecular biology of the Bunyaviridae. Journal of General Virology 71, 501–522.

Elliott, R.M., Bouloy, M., Calisher, C.H., Goldbach, R., Moyer, J.T., Nichol, S.T., Petterson, R., Plyusin, A., Schmaljohn, C., 2000. Bunyaviridae. In: van Regenmortel, C.M.F.M.H.V., Bishop, D.H.L., Carstens, E.B., Estes, M.K., Lemon, S.M., Maniloff, J., Mayo, M.A., McGeoch, D.J., Pringle, C.R., Wickner, R.B. (Eds.), Virus Taxonomy: The Classification and Nomenclature of Viruses. Seventh Report of the International Committee on Taxonomy of Viruses. Academic Press, San Diego, pp. 599–621.

Gott, P., Zoller, L., Darai, G., Bautz, E.K., 1997. A major antigenic domain of hantaviruses is located on the aminoproximal site of the viral nucleocapsid protein. Virus Genes 14, 31–40.

Hjelle, B., Jenison, S., Torrez-Martinez, N., Yamada, T., Nolte, K., Zumwalt, R., MacInnes, K., Myers, G., 1994. A novel hantavirus associated with an outbreak of fatal respiratory disease in the southwestern United States: evolutionary relationships to known hantaviruses. Journal of Virology 68, 592–596.

Hughes, A.L., Friedman, R., 2000. Evolutionary diversification of protein-coding genes of hantaviruses. Molecular Biology and Evolution 17, 1558–1568.

Jonsson, C.B., Figueiredo, L.T., Vapalahti, O., 2010. A global perspective on hantavirus ecology, epidemiology, and disease. Clinical Microbiology Reviews 23, 412–441.

Kariwa, H., Yoshida, H., Sanchez-Hernandez, C., Romero-Almaraz Mde, L., Almazan-Catalan, J.A., Ramos, C., Miyashita, D., Seto, T., Takano, A., Totani, M., Murata, R., Saasa, N., Ishizuka, M., Sanada, T., Yoshii, K., Yoshimatsu, K., Arikawa, J., Takashima, I., 2012. Genetic diversity of hantaviruses in Mexico: identification of three novel hantaviruses from Neotominae rodents. Virus Research 163, 486–494.

Kariwa, H., Yoshimatsu, K., Arikawa, J., 2007. Hantavirus infection in East Asia. Comparative Immunology, Microbiology and Infectious Diseases 30, 341–356.

Kaukinen, P., Koistinen, V., Vapalahti, O., Vaheri, A., Plyusnin, A., 2001. Interaction between molecules of hantavirus nucleocapsid protein. Journal of General Virology 82, 1845–1853.

Kaukinen, P., Kumar, V., Tulimaki, K., Engelhardt, P., Vaheri, A., Plyusnin, A., 2004. Oligomerization of Hantavirus N protein: C-terminal alpha-helices interact to form a shared hydrophobic space. Journal of Virology 78, 13669–13677.

Koma, T., Yoshimatsu, K., Pini, N., Safronetz, D., Taruishi, M., Levis, S., Endo, R., Shimizu, K., Yasuda, S.P., Ebihara, H., Feldmann, H., Enria, D., Arikawa, J., 2010. Truncated hantavirus nucleocapsid proteins for serotyping Sin Nombre, Andes, and Laguna Negra hantavirus infections in humans and rodents. Journal of Clinical Microbiology 48, 1635–1642.

Lee, H.W., van der Groen, G., 1989. Hemorrhagic fever with renal syndrome. Progress in Medical Virology 36, 62–102.

Lundkvist, A., Fatouros, A., Niklasson, B., 1991. Antigenic variation of European haemorrhagic fever with renal syndrome virus strains characterized using bank vole monoclonal antibodies. Journal of General Virology 72, 2097–2103.

Maes, P., Klempa, B., Clement, J., Matthijnssens, J., Gajdusek, D.C., Kruger, D.H., Van Ranst, M., 2009. A proposal for new criteria for the classification of hantaviruses, based on S and M segment protein sequences. Infection, Genetics and Evolution 9, 813–820.

Meyer, B.J., Schmaljohn, C.S., 2000. Persistent hantavirus infections: characteristics and mechanisms. Trends in Microbiology 8, 61–67.

Morii, M., Yoshimatsu, K., Arikawa, J., Zhou, G., Kariwa, H., Takashima, I., 1998. Antigenic characterization of Hantaan and Seoul virus nucleocapsid proteins expressed by recombinant baculovirus: application of a truncated protein, lacking an antigenic region common to the two viruses, as a serotyping antigen. Journal of Clinical Microbiology 36, 2514–2521.

Nakamura, I., Yoshimatsu, K., Lee, B.H., Okumura, M., Taruishi, M., Araki, K., Kariwa, H., Takashima, I., Arikawa, J., 2008. Development of a serotyping ELISA system for Thailand virus infection. Archives of Virology 153, 1537–1542.

Okumura, M., Yoshimatsu, K., Araki, K., Lee, B.H., Asano, A., Agui, T., Arikawa, J., 2004. Epitope analysis of monoclonal antibody E5/G6, which binds to a linear epitope in the nucleocapsid protein of hantaviruses. Archives of Virology 149, 2427–2434.

Perriere, G., Gouy, M., 1996. WWW-query: an on-line retrieval system for biological sequence banks. Biochimie 78, 364–369.

Peters, C.J., Khan, A.S., 2002. Hantavirus pulmonary syndrome: the new American hemorrhagic fever. Clinical Infectious Diseases 34, 1224–1231.

Ravkov, E.V., Rollin, P.E., Ksiazek, T.G., Peters, C.J., Nichol, S.T., 1995. Genetic and serologic analysis of Black Creek Canal virus and its association with human disease and Sigmodon hispidus infection. Virology 210, 482–489.

Ruo, S.L., Sanchez, A., Elliott, L.H., Brammer, L.S., McCormick, J.B., Fisher, H.-S., 1991. Monoclonal antibodies to three strains of hantaviruses: Hantaan, R22, and Puumala. Archives of Virology 119, 1–11.

Schmaljohn, C., Hjelle, B., 1997. Hantaviruses: a global disease problem. Emerging Infectious Diseases 3, 95–104.

Schmaljohn, C.S., 1996. Molecular biology of hantaviruses. In: Elliott, R.M. (Ed.), The Bunyaviridae. Plenum Press, New York, pp. 63–90.

Tischler, N.D., Rosemblatt, M., Valenzuela, P.D., 2008. Characterization of cross-reactive and serotype-specific epitopes on the nucleocapsid proteins of hantaviruses. Virus Research 135, 1–9.

Vapalahti, O., Kallio-Kokko, H., Narvanen, A., Julkunen, I., Lundkvist, A., Plyusnin, A., Lehvaslaiho, H., Brummer-Korvenkontio, M., Vaheri, A., Lankinen, H., 1995. Human B-cell epitopes of Puumala virus nucleocapsid protein, the major antigen in early serological response. Journal of Medical Virology 46, 293–303.

Yamada, T., Hjelle, B., Lanzi, R., Morris, C., Anderson, B., Jenison, S., 1995. Antibody responses to Four Corners hantavirus infections in the deer mouse (*Peromyscus maniculatus*): identification of an immunodominant region of the viral nucleocapsid protein. Journal of Virology 69, 1939–1943.

Yasuda, S.P., Yoshimatsu, K., Koma, T., Shimizu, K., Endo, R., Isozumi, R., Arikawa, J., 2012. Application of truncated nucleocapsid protein (N) for serotyping ELISA of murinae-associated hantavirus infection in rats. Journal of Veterinary Medical Science 74, 215–219.

Yoshimatsu, K., Arikawa, J., Kariwa, H., 1993. Application of a recombinant baculovirus expressing hantavirus nucleocapsid protein as a diagnostic antigen in IFA test: cross reactivities among 3 serotypes of hantavirus which causes

hemorrhagic fever with renal syndrome (HFRS). Journal of Veterinary Medical Science 55, 1047–1050.
Yoshimatsu, K., Arikawa, J., Tamura, M., Yoshida, R., Lundkvist, A., Niklasson, B., Kariwa, H., Azuma, I., 1996. Characterization of the nucleocapsid protein of Hantaan virus strain 76-118 using monoclonal antibodies. Journal of General Virology 77, 695–704.
Yoshimatsu, K., Arikawa, J., Yoshida, R., Li, H., Yoo, Y.C., Kariwa, H., Hashimoto, N., Kakinuma, M., Nobunaga, T., Azuma, I., 1995. Production of recombinant hantavirus nucleocapsid protein expressed in silkworm larvae and its use as a diagnostic antigen in detecting antibodies in serum from infected rats. Laboratory Animal Science 45, 641–646.
Yoshimatsu, K., Lee, B.H., Araki, K., Morimatsu, M., Ogino, M., Ebihara, H., Arikawa, J., 2003. The multimerization of hantavirus nucleocapsid protein depends on type-specific epitopes. Journal of Virology 77, 943–952.
Zeier, M., Handermann, M., Bahr, U., Rensch, B., Muller, S., Kehm, R., Muranyi, W., Darai, G., 2005. New ecological aspects of hantavirus infection: a change of a paradigm and a challenge of prevention – a review. Virus Genes 30, 157–180.

Virus Research 165 (2012) 34–45

Contents lists available at SciVerse ScienceDirect

Virus Research

journal homepage: www.elsevier.com/locate/virusres

Serial passage of a street rabies virus in mouse neuroblastoma cells resulted in attenuation: Potential role of the additional *N*-glycosylation of a viral glycoprotein in the reduced pathogenicity of street rabies virus☆

Kentaro Yamada[a], Chun-Ho Park[b], Kazuko Noguchi[c], Daisuke Kojima[b], Tatsuya Kubo[b], Naoyuki Komiya[b], Takashi Matsumoto[c], Marcelo Takahiro Mitui[c], Kamruddin Ahmed[a], Kinjiro Morimoto[d], Satoshi Inoue[e], Akira Nishizono[a,c,*]

[a] *Research Promotion Project, Oita University, 1-1 Idaigaoka, Hasama-machi, Yufu, Oita 879-5593, Japan*
[b] *Department of Veterinary Pathology, School of Veterinary Medicine, Kitasato University, 23-35-1 Higashi, Towada, Aomori 034-8628, Japan*
[c] *Department of Microbiology, Faculty of Medicine, Oita University, 1-1 Idaigaoka, Hasama-machi, Yufu, Oita 879-5593, Japan*
[d] *Department of Medical Pharmacy, Faculty of Pharmacy, Yasuda Women's University, Hiroshima 731-0153, Japan*
[e] *Department of Veterinary Science, National Institute of Infectious Diseases, Toyama 1-23-1, Shinjuku, Tokyo 162-8640, Japan*

ARTICLE INFO

Article history:
Received 10 September 2011
Received in revised form
23 December 2011
Accepted 1 January 2012
Available online 11 January 2012

Keywords:
Street rabies virus
Serial passage
Glycoprotein
N-Glycosylation
Adaptation
Pathogenicity

ABSTRACT

Street rabies viruses are field isolates known to be highly neurotropic. However, the viral elements related to their pathogenicity have yet to be identified at the nucleotide or amino acid level. Here, through 30 passages in mouse neuroblastoma NA cells, we have established an attenuated variant of street rabies virus strain 1088, originating from a rabid woodchuck followed by 2 passages in the brains of suckling mice. The variant, 1088-N30, was well adapted to NA cells and highly attenuated in adult mice after intramuscular (i.m.) but not intracerebral (i.c.) inoculations. 1088-N30 had seven nucleotide substitutions, and the R196S mutation of the G protein led to an additional *N*-glycosylation. Street viruses usually possess one or two *N*-glycosylation sites on the G protein, 1088 has two, while an additional *N*-glycosylation site is observed in laboratory-adapted strains. We also established a cloned variant 1088-N4#14 by limiting dilution. Apart from the R196S mutation, 1088-N4#14 possessed only one amino acid substitution in the P protein, which is found in several field isolates. 1088-N4#14 also efficiently replicated in NA cells and was attenuated in adult mice after i.m. inoculations, although it was more pathogenic than 1088-N30. The spread of 1088-N30 in the brain was highly restricted after i.m. inoculations, although the pattern of 1088-N4#14's spread was intermediate between that of the parental 1088 and 1088-N30. Meanwhile, both variants strongly induced humoral immune responses in mice compared to 1088. Our results indicate that the additional *N*-glycosylation is likely related to the reduced pathogenicity. Taken together, we propose that the number of *N*-glycosylation sites in the G protein is one of the determinants of the pathogenicity of street rabies viruses.

© 2012 Elsevier B.V. All rights reserved.

1. Introduction

Rabies virus is a causative agent of rabies, a fatal encephalitis in mammals, including humans. Rabies viruses belong to the genus *Lyssavirus*, family *Rhabdoviridae*. They are bullet-shaped enveloped viruses and have a nonsegmented negative-strand RNA genome about 12 kb in length. The genome encodes five viral proteins: the nucleoprotein (N), phosphoprotein (P), matrix protein (M), glycoprotein (G), and large protein (L). The G protein is the only viral protein that is glycosylated and exposed at the surface of the virion (Wunner, 2007). It is also responsible for the interaction with receptors to enter into target cells and the induction of a humoral immune response, such as the production of virus-neutralizing antibodies (Wunner, 2007). Moreover, studies show that the G protein is the major factor responsible for the

Abbreviations: BBB, blood–brain barrier; CNS, central nervous system; CVS, challenge virus standard; DMEM, Dulbecco's modified Eagle's medium; EMEM, Eagle's minimum essential medium; ER, endoplasmic reticulum; ERAD, ER-associated degradation; FCS, fetal calf serum; FFU, focus-forming units; i.c., intracerebral; i.m., intramuscular; IU, international units; LD_{50}, 50% lethal dose; MAb, monoclonal antibody; MOI, multiplicity of infection; p.i., post-inoculation; SD, standard deviation; SHBRV, silver-haired bat rabies virus; USA, United States of America; VNA, virus neutralizing antibodies; WNV, West Nile virus.

☆ The sequences determined in the present study have been deposited in the GenBank/EMBL/DDBJ databases (GenBank ID: AB645847).

* Corresponding author at: Department of Microbiology, Faculty of Medicine, Oita University, 1-1 Idaigaoka, Hasama-machi, Yufu, Oita 879-5593, Japan.
Tel.: +81 97 586 5710; fax: +81 97 586 5719.
E-mail address: a24zono@oita-u.ac.jp (A. Nishizono).

0168-1702/$ – see front matter © 2012 Elsevier B.V. All rights reserved.
doi:10.1016/j.virusres.2012.01.002

pathogenesis of rabies viruses (Dietzschold et al., 1983, 1985; Etessami et al., 2000; Ito et al., 2001b; Morimoto et al., 1999, 2000; Seif et al., 1985; Takayama-Ito et al., 2004, 2006a,b; Tuffereau et al., 1989).

Rabies viruses are generally classified into two categories, street viruses (field isolates) and fixed viruses (laboratory-adapted strains). Street viruses are known to be more pathogenic than fixed viruses after peripheral infections. The first fixed virus was established by Pasteur through the repeated passaging of a street virus in rabbits via intracerebral (i.c.) inoculations (Baer, 2007; Lepine, 1938). Although fixed viruses are generally neurovirulent (pathogenic to animals after an i.c. inoculation), they have different characteristics from street viruses, such as regularity and shortening of the incubation period, stabilization of virulence, and a reduction or loss of infectivity after peripheral inoculations (Lepine, 1938).

Some groups have investigated the pathogenecity of street viruses using the silver-haired bat-associated rabies virus (SHBRV), a highly pathogenic and neuroinvasive street virus (Dietzschold et al., 2000). Compared to attenuated fixed strains, SHBRV is a poor inducer of innate immune responses in mice after an intramuscular (i.m.) inoculation (Wang et al., 2005), and mice infected with SHBRV intradermally failed to open the blood–brain barrier (BBB) and to recruit immune effectors into the CNS (Roy and Hooper, 2007; Roy et al., 2007). The maintenance of the BBB permeability was also observed for several terrestrial animal-derived viruses (Kuang et al., 2009; Roy and Hooper, 2008). In addition, the study of chimeric viruses generated from SHBRV and the fixed virus SAD B19 has been identified the M and G proteins as related to the pathogenecity of SHBRV; the M and G proteins enhanced viral internalization and spread in cultured cells (Faber et al., 2004; Pulmanausahakul et al., 2008). However, viral elements such as domains, motifs, and amino acid residues, involved in the pathogenesis of street viruses have yet to be identified. One reason for this is that most studies were performed with fixed strains although the genetic similarity between street and fixed strains is not very high.

The number of *N*-glycosylation sites in the G protein might be related to the difference between street and fixed viruses. Several fixed viruses have three or four potential glycosylation sites on the G protein, and most have two sequons, Asn at positions 37 and 319 (Asn^{37} and Asn^{319}) (Morimoto et al., 1992). Recently, Ming et al. (2009) mentioned that the Chinese street virus HN10 has only two sequons at Asn^{37} and Asn^{319}, and that the sequon at Asn^{247}, which is present in many fixed viruses, is absent in other street viruses as well. Interestingly, in the West Nile virus (WNV), *N*-glycosylation of the envelope (E) protein is responsible for neuroinvasiveness and growth efficiency in cells (Beasley et al., 2005; Shirato et al., 2004). However, there is as yet no direct evidence for the impact of *N*-glycosylation on the rabies virus' biological activity.

Parasites, including viruses, are attenuated after serial passaging in cell cultures (Ebert, 1998). Interestingly, several attenuated fixed rabies viruses regained neurovirulence (killing adult mice after i.c. inoculations) after a few passages in murine or human neuroblastoma cell lines (Clark, 1978). Therefore, since we suspected that the neurovirulence of rabies viruses is maintained during serial passaging in mouse neuroblastoma NA cells, in this study we have attempted to establish an attenuated street virus variant by serial passage of strain 1088 in NA cells in order to identify the viral element(s) responsible for the pathogenecity of street viruses other than neurovirulence. We obtained an NA cell-adapted variant, which was attenuated in mice after i.m. but not i.c. inoculations. This variant had only seven nucleotide substitutions compared to the parental strain, one of which led to additional *N*-glycosylation of the G protein. Furthermore, we established a cloned variant, the G protein of which possessed the single mutation. This variant was also adapted to NA cells and attenuated in mice after i.m. inoculations. Hence, we propose that the additional *N*-glycosylation of the G protein is likely related to the adaptation to NA cells and attenuation of the pathogenicity of street rabies viruses.

2. Materials and methods

2.1. Cell and virus

Mouse neuroblastoma C1300 (NA) cells were grown in Eagle's minimal essential medium (EMEM) supplemented with 10% fetal calf serum (FCS), penicillin (100 U/ml) and streptomycin (100 μg/ml). Street rabies virus 1088, a strain isolated from a woodchuck in the Centers for Disease Control in Atlanta, USA was obtained from the Yale Arbovirus Unit, Yale University (Mifune et al., 1979). The strain was passaged in the brains of suckling mice only twice since the original isolation. The supernatant of the 10% brain homogenate was used.

2.2. Serial passage

Monolayered NA cells in 6-well plates, T-75 flasks, or T-25 flasks were used for the serial passage of strain 1088. Until the 24th passage, each virus stock was diluted 10-fold with EMEM containing 2% FCS and inoculated into NA cells at 150 μl per well in 6-well plates, 500 μl in T-25 flasks, or 1 ml in T-75 flasks. After the 25th passage, the virus was diluted 100- or 1000-fold with EMEM containing 2% FCS. After adsorption for 1 h at 37 °C, the inoculum was removed, and Dulbecco's modified Eagle's medium (DMEM) containing 5% FCS was added at 2.5 ml per well in 6-well plates, 5 ml in T-25 flasks, or 15 ml in T-75 flasks. The inoculated cells were incubated at 37 °C for several days. When about 50% of the cells were detached, the medium was collected and centrifuged at 2000 × *g* and 4 °C to remove debris. The supernatant was collected and stored at −80 °C until used.

2.3. Virus titration

The virus was titrated by a focus assay on confluent monolayers of NA cells in 24-well plates. Serial 10-fold dilutions of virus were made with EMEM containing 2% FCS and then 100 μl of each dilution was inoculated into the cells in quadruplicate. After 1 h at 37 °C, the cells were washed twice with Hanks' balanced salt solution. Subsequently, the cells were overlaid with EMEM containing 5% FCS and 1% (w/v) methylcellulose (catalog no. M0512, SIGMA) and then incubated at 37 °C. At 4 days post-inoculation (p.i.), the cells were fixed with 4% paraformaldehyde and permeabilized with 0.2% Triton X-100 in phosphate-buffered saline (PBS). Subsequently, the cells were stained with FITC Anti-Rabies Monoclonal Globulin (Fujirebio Diagnostics, Inc.). Viral foci were counted under an inverted fluorescent microscope, and the viral titer was expressed as focus-forming units (FFU).

2.4. Nucleotide sequence analysis

Viral RNA was isolated from a virus stock or cells using Trizol reagent (Invitrogen). Subsequently, cDNA was synthesized using random hexamers and SuperScript III reverse transcriptase (Invitrogen). PCR was performed with Ex-Taq (Takara Bio inc., Japan). The 3′ and 5′ ends of the viral genome were amplified from total RNA of virus-inoculated cells by 5′-RACE (rapid amplification of cDNA ends) using the SMART RACE cDNA Amplification Kit (Clontech) following the manufacturer's instructions. The amplified DNA fragment was purified using a Nucleospin Extract II kit (Macherey-Nagel) and then the DNA sequence was determined using BigDye Terminator ver. 3.1 and the ABI 3130 Genetic Analyzer

(Applied Biosystems). The sequences obtained were analyzed with GENETYX-MAC software ver. 15 (Genetyx corp., Japan). Detailed information of primers used is available from the authors on request. The complete genome sequence of strain 1088 determined in this study has been deposited in DDBJ/EMBL/GenBank (GenBank ID: AB645847).

2.5. Virus cloning by limiting dilution

The *N*-glycosylation variant of 1088 was cloned from the stock of the fourth passage by limiting dilution as follows. The stock was diluted to 2.5 FFU/ml and 200 μl of the diluted solution was added to monolayered NA cells in 12-well plates (0.5 FFU/well). After adsorption for 1 h, the inocula were removed and 3 ml of DMEM containing 5% FCS was added to the cells. The inoculated cells were incubated at 37 °C. At 11 days p.i., the culture medium was collected and stored at −80 °C. Simultaneously, the cells were processed for Western blotting as described below. After the mobility of the G proteins of the clones was checked by Western blotting, the positive clone was propagated twice in NA cells and then the entire genome was sequenced as described above. Finally, we chose one clone, named 1088-N4#14.

2.6. Plasmid construction

An expression vector for the 1088 (N0) G or variant (1088-N4#14 or 1088-N30) G was constructed as follows. Each G gene was amplified from the corresponding cDNA by PCR with KOD Plus ver. 2 (Toyobo, Japan) using the primers EcoRI-1088-Gf (5′-AACCGGAATTCCACCATGGTTCCTCAGGCTCTT-3′; EcoRI site is underlined) and XbaI-1088-Gr (5′-AAAGCTCTAGATTCAC-AGACTGGTCTCACC-3′; XbaI site is underlined). The DNA fragment was cloned into the pCI vector (Promega) after digestion with EcoRI and XbaI. Newly constructed plasmids were sequenced for verification.

2.7. Tunicamycin treatment

NA cells were inoculated with each virus at a multiplicity of infection (MOI) of 1 and then incubated in the absence or presence (1 μg/ml) of tunicamycin (Sigma–Aldrich). At 28 h p.i., the cells were processed for Western blotting as described below.

The plasmid encoding the G protein (0.5 μg/well) was transfected into NA cells in 24-well plates using TransIT-Neural reagent (Mirus) according to the manufacturer's instructions. At 4 h post-transfection, the medium was replaced with EMEM containing 10% FCS with or without 1 μg/ml tunicamycin. After additional incubation for 20 h, the transfected cells were processed for Western blotting.

2.8. Western blotting

Cells were lysed with a lysis buffer [50 mM Tris–HCl (pH 8.0), 1% NP-40 and 150 mM NaCl], and then mixed with the same amount of 2× sodium dodecyl sulfate-polyacrylamide gel electrophoresis (SDS-PAGE) sample buffer [125 mM Tris–HCl (pH 6.8), 4% SDS, 10% (w/v) sucrose, 10% (v/v) 2-mercaptoethanol and 0.01% (w/v) bromophenol blue]. After incubation at 95 °C for 5 min, proteins in the samples were separated by SDS-PAGE in a 10% gel and then transferred onto a polyvinylidene difluoride (PVDF) membrane (0.45 μm; Millipore) for analysis by Western blotting. After blocking with PBS containing 5% skim milk and 0.1% Tween-20, the membrane was incubated with the anti-G mouse monoclonal antibody (MAb) 15-13 (Luo et al., 1998), anti-N mouse MAb 8-1 (Minamoto et al., 1994), or anti-β-actin mouse MAb G043 (Applied Biological Materials Inc., Canada) in PBS containing 2.5% skim milk and 0.1% Tween-20. After being washed with PBS containing 0.1% Tween-20, the membrane was incubated with peroxidase-conjugated anti-mouse IgG (Cappel) in PBS containing 2.5% skim milk and 0.1% Tween-20. Protein bands were visualized using SuperSignal West Femto Maximum Sensitivity Substrate (Thermo Fisher Scientific).

2.9. Virus growth in NA cells

Monolayered NA cells in 24-well plates were inoculated with each virus at an MOI of 0.01 or 1. After adsorption for 1 h, the cells were washed twice with Hanks' balanced salt solution and resupplied with 1 ml of EMEM containing 5% FCS per well. The cells were incubated at 37 °C and samples of the culture medium were harvested at 24, 48, 72, and 96 h p.i. Each sample was centrifuged at 800 × *g* for 10 min, and its supernatant was stored at −80 °C. The viral titer in a sample was determined in NA cells as described above. In addition, the remaining cells were processed for Western blotting as described above.

2.10. Pathogenicity of viruses in adult mice

Six-week-old female ddY mice (Kyudo Co. Ltd., Japan) were used. Serial 10-fold dilutions of each virus were made with PBS containing 2% FCS. Subsequently, 0.03 ml of each dilution was injected i.c. into groups of five mice. Meanwhile, 0.05 ml of each dilution was injected by i.m. (right hindlimb of mice). The inoculated mice were weighted every day and observed for 28 or 42 days after the i.c. or i.m. injection, respectively. The 50% lethal dose (LD_{50}) was calculated by the method of Reed and Müench (1938). All animal experiments were performed with the approval of the ethics committee of Oita University.

2.11. Immunohistochemistry

Fifteen ddY mice (6-week-old, female) per group were inoculated with 10^6 FFU of each strain. At 5, 8 and 11 days p.i., five mice per group were sacrificed and their sera, tissues and organs were sampled. The tissues and organs were fixed with a 10% Formalin Neutral Buffer Solution (Wako, Japan). Immunohistochemistry with brain sections embedded in paraffin was performed using the anti-P rabbit serum (Shoji et al., 2004) as described previously (Kojima et al., 2010).

2.12. Rapid fluorescent focus inhibition tests

Viral neutralizing antibodies (VNA) against the rabies virus were determined by rapid fluorescent focus inhibition tests (RFFIT) as described previously (Shiota et al., 2009; Smith et al., 1973). VNA titers were represented as international units per ml (IU/ml), which was calculated by comparison with WHO international standards [RAI: Anti-rabies Immunoglobulin, human, National Institute for Biological Standards & Control (NIBSC)].

2.13. Virus internalization assay

Monolayered NA cells in 24-well plates were incubated with approx 120 FFUs of each virus per well for several time periods (10, 20, 40, 60, and 80 min) at 37 °C. The cells were then washed twice with Hanks' balanced salt solution and overlaid with EMEM containing 5% FCS and 1% (w/v) methylcellulose. The cells were incubated at 37 °C for 4 days, and viral foci were visualized as described above. The efficiency with which each virus was internalized is expressed as the relative number of foci, with the number at 80 min as 100%.

2.14. Fusion assay

NA cells in 48-well plates were transfected with 0.25 μg of the pCI vector encoding the G protein or pCI empty vector using TransIT-Neural according to the manufacturer's instructions. After 2 days post-transfection, cells were rinsed with each fusion medium, EMEM containing 10 mM 2-morpholinoethanesulfonic acid monohydrate (MES) and 10 mM N-2-hydroxyethyl-piperazine N′-2-ethanesulfonic acid (HEPES), adjusted to pH 5.8, 6.0 or 6.2 and replenished with the same fusion medium. After incubation at 37 °C for 30 min, cells were fixed with 4% paraformaldehyde and then stained with fuchsine solution. Images were obtained using BIOREVO BZ-9000 (Keyence, Japan).

3. Results

3.1. Adaptation of street virus 1088 to NA cells after serial passaging

We performed the serial passage of 1088 in NA cells. In the first passage, the titer was only 2×10^5 FFU/ml although the cells were inoculated with 1088, hereafter 1088 (N0), at an MOI of 1. Meanwhile, at the 30th passage, the titer reached 10^8 FFU/ml. Then, the virus passaged 30 times, 1088-N30, was used for further analysis as an NA cell-adapted 1088 variant.

3.2. 1088-N30 had seven nucleotide substitutions

We compared the overall genomic sequences of 1088 (N0) and 1088-N30. Both genomes were 11,923 nucleotides (nt) in length, the same as several street viruses (Delmas et al., 2008; Faber et al., 2004; Ming et al., 2009; Szanto et al., 2008). Seven nucleotide substitutions were observed between the two viruses (Table 1). One nucleotide ambiguity was observed at nt 2513 of the 1088 (N0) genome, and three ambiguities were detected at nt 17, 28, and 1187 of the 1088-N30 genome. Three substitutions were detected in the non-coding region but not located in any known functional regions, such as start and stop signals for viral mRNA transcription. Three of four substitutions in the coding regions led to amino acid changes; two changes were located in the G protein. Of these, the change at position 196 from arginine to serine (R196S) led to the additional sequon at Asn^{194} (from Asn^{194}-Ser^{195}-Arg^{196} to Asn^{194}-Ser^{195}-Ser^{196}). *N*-Glycosylation typically occurs at the sequon Asn-X-Ser/Thr, where X is any amino acid except Pro. In addition, the amino acid at 333 of the G protein, one of the determinants of the virulence of the fixed viruses (Dietzschold et al., 1983; Seif et al., 1985; Takayama-Ito et al., 2006a; Tuffereau et al., 1989), did not change during the serial passage and was a virulent type Arg in both viruses.

3.3. Emergence of the R196S mutation corresponds to the increasing viral titer during serial passage

To determine when the mutations occurred, we examined nucleotide sequences during the series of passages. As shown in Fig. 1, the R196S mutation (A to T) emerged in the fourth passage, interestingly corresponding to the increase in the viral titer in NA cells. The T nucleotide became dominant in the sixth passage, whereas the A nucleotide was not detected in the ninth passage. Conversely, the P144L mutation in the G protein emerged in the seventh passage. At the site detected as ambiguous in the M gene (nt 2513), the A nucleotide was dominant in the 1088 (N0) genome (Table 1), but the G nucleotide became dominant in the seventh passage (data not shown). In addition, the mutation did not lead to an amino acid change. The other mutations occurred after the 14th passage (data not shown). Therefore, out of the mutations detected in the 1088-N30 genome, R196S was the first amino acid change and likely responsible for the adaptation to NA cells.

3.4. Cloning of the 1088 R196S variant

To obtain a 1088 variant that possesses only the R196S mutation in the G protein, we attempted cloning by limiting dilution from the virus stock of the fourth passage as described in Materials and methods. We picked out a clone designated 1088-N4#14 for further analysis. We determined the whole genome sequence of 1088-N4#14 and compared it with that of the 1088 (N0). In addition to R196S, the 1088-N4#14 genome had a mutation which leads to an amino acid substitution at position 61 from glycine to glutamate (G61E) in the P protein (Table 1). As the G61E mutation was also observed in several field isolates from terrestrial animals in the Americas (GenBank ID: AF369289, AF369308, AF369313, AF369323, AF369337, and AY998275), it probably does not affect the pathogenicity of street viruses.

3.5. In vitro characterization of 1088 and the 1088 variants

We examined the in vitro biological properties of 1088 (N0) and the 1088 variants. Initially, we checked the *N*-glycosylation status of the G protein (Fig. 2A). In the absence of the *N*-glycosylation inhibitor tunicamycin, both variant G proteins had less mobility than the 1088 (N0) G protein. In the presence of tunicamycin, the 1088-N30 G protein showed almost the same mobility as the 1088 (N0) G protein. A similar result was obtained when the G protein was expressed by a plasmid vector (Fig. 2B). Therefore, the R196S mutation solely leads to the additional *N*-glycosylation of the G protein.

Next, the growth kinetics of 1088 (N0) and the 1088 variants in NA cells were determined (Fig. 3A). At an MOI of 0.01, the 1088 variants replicated significantly better than 1088 (N0); their titers were four orders of magnitude higher than that of 1088 at 4 days p.i. Even at an MOI of 1, the 1088 variants replicated significantly better than 1088 (N0); the titers of 1088-N4#14 and 1088-N30 were three and two orders of magnitude higher than that of 1088 (N0) at 4 days p.i., respectively. These results indicate that 1088-N4#14 also adapted to NA cells as well as 1088-N30.

In addition, we determined the expression levels of the viral proteins in the MOI of 1 inoculation (Fig. 3B). Expression levels of the N protein increased in a time-dependent manner. Surprisingly, the levels were similar between the three viruses although the titers of 1088 (N0) were significantly lower than those of the variants (Fig. 3A). The G protein expression also increased in a time-dependent manner, however, the G protein was detected at low levels in the 1088-N30 infection compared with the 1088 (N0) and 1088-N4#14 infections throughout the indicated time points. Northern blot analysis revealed the mRNA expression of the G gene of 1088-30 to be at least as high as that of 1088 (N0) and 1088-N4#14 (Supplementary Fig. 1), indicating that the lower levels of the G protein of 1088-N30 were due to post-transcriptional events in the infected NA cells. In conclusion, the difference in the production of progeny viruses did not depend on the expression levels of viral proteins within the infected cells.

3.6. Both 1088 variants were attenuated in adult mice after intramuscular, but not intracerebral, inoculations

The pathogenicity of the three viruses was assessed in adult mice. After i.c. inoculations, both variants killed the adult mice as effectively as 1088 (N0), and the LD_{50} values of 1088 (N0), 1088-N4#14, and 1088-N30 were nearly identical (6.8, 6.8, and 5.0 FFU, respectively). Thus, 1088-N4#14 and 1088-N30 were not attenuated in neurovirulence in adult mice.

Table 1
Sequence differences between 1088 (N0), 1088-N4#14, and 1088-N30.

Nucleotide position	Region	Amino acid position	Nucleotide (amino acid)		
			1088 (N0)	1088-N4#14	1088-N30
17	Leader		T	T	T/C[a]
28	Leader		G	G	G/A[a]
1187	N gene	373	G (Glu)	G (Glu)	G/A[a] (Glu/Lys)
1695	P gene	61	G (Gly)	A (Glu)	G (Gly)
2513	M gene	6	A/G[b] (Lys)	A(Lys)	G (Lys)
3803	G gene	144	C (Pro)	C (Pro)	T (Leu)
3960	G gene	196	A (Arg)	T (Ser)	T (Ser)
11870	Trailer		A	A	G

[a] Signal strength was almost identical.
[b] The signal for the A nucleotide was dominant.

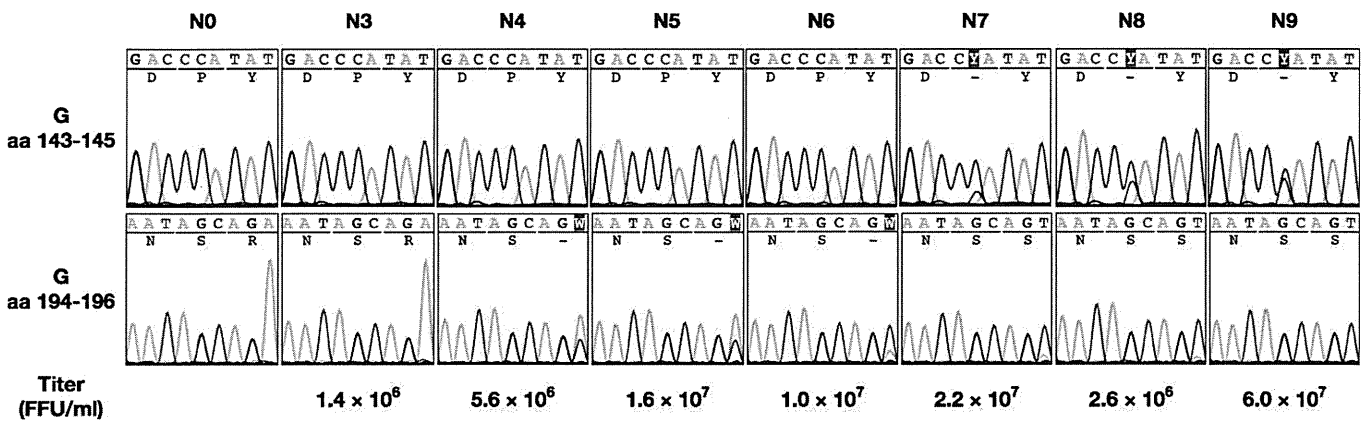

Fig. 1. Mutational events in the G gene during serial passaging. Sequence electropherograms of the G gene (amino acid regions from residues 143 to 145 and from residues 194 to 196) were obtained by RT-PCR and direct sequencing of virus stocks at the indicated passages. A titer in the supernatant for each passage is shown of the bottom.

Subsequently, we inoculated adult mice with serial dilutions (10^3–10^6 FFU) of each virus via the i.m. route (Table 2). At 10^6 FFU, all mice died from the 1088 (N0) infection, but all mice survived the 1088-N30 infection. Meanwhile, half of the mice survived the 1088-N4#14 infection. In total, 75% of mice inoculated with 1088 (N0) died, compared to only 10% of mice inoculated with 1088-N30. In the 1088-N4#14 infection, 30% of mice died in total, and a value intermediate between those for the 1088 (N0) and 1088-N30 infections. Therefore, 1088-N4#14 and 1088-N30 had reduced pathogenicity after the i.m. inoculation in adult mice although 1088-N4#14 showed moderate attenuation.

3.7. Distribution of viral antigens and humoral immune response in mice inoculated via the i.m. route

In order to investigate the events within the mice inoculated i.m., we prepared adult mice inoculated with each virus at 10^6 FFU and then collected serum, tissue and organ samples from five mice

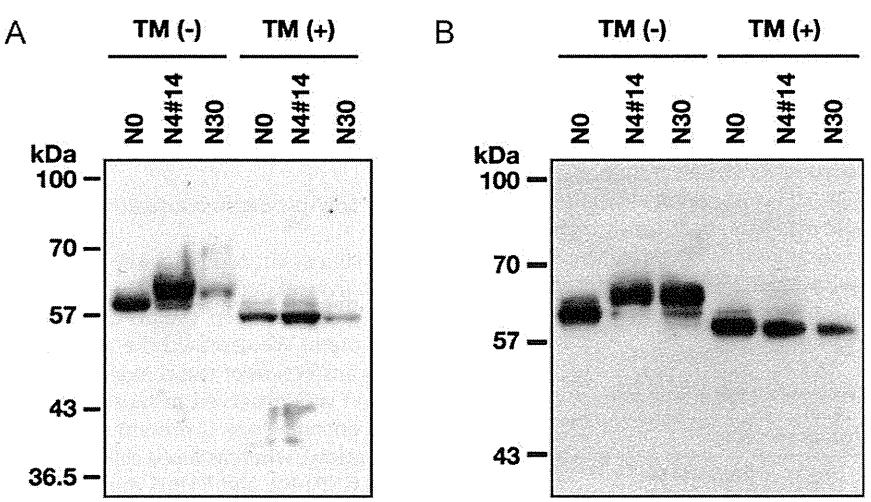

Fig. 2. *N*-Glycosylation of the G protein. Each virus was inoculated at an MOI of 1 (A), or each plasmid encoding the G protein was transfected into NA cells (B). The inoculated or transfected cells were incubated in the absence (−) or presence (+) of tunicamycin (TM, 1 μg/ml). The G proteins in the cells were detected by Western blotting using the anti-G antibody.

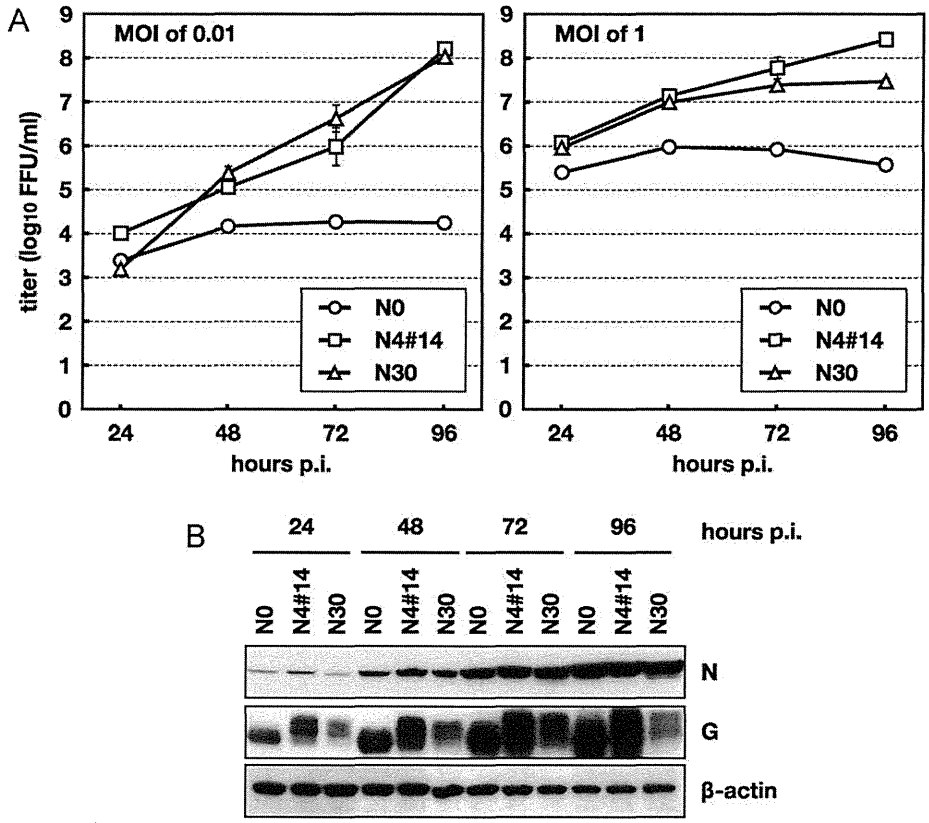

Fig. 3. (A) Virus growth curves in NA cells. Each virus was inoculated at an MOI of 0.01 or 1, and samples were collected at 24, 48, 72, and 96 h p.i. Titers represent the mean and standard deviation (SD) for three wells. (B) Viral proteins expressed in the infected NA cells at an MOI of 1. Lysates of the infected cells were prepared at the indicated time points, and viral proteins (N and G proteins) and β-actin were detected by Western blotting. 1088, (N0); 1088-N4#14, (N4#14); 1088-N30, (N30).

each at 5, 8, and 11 days p.i. after euthanasia. The viral spread within the CNS was examined by immunohistochemistry (Fig. 4A). At 5 days p.i., viral antigen-positive cells were detected in brain cortices, indicating that both 1088 variants were still neuroinvasive. At 8 and 11 days p.i., the viral antigen was widely distributed throughout the brain in the 1088 (N0)-infected mice. In contrast, its distribution was highly restricted in the 1088-N30-inoculated mice. Conversely, the distribution patterns for the 1088-N4#14 infection were intermediate between those for the 1088 (N0) and 1088-N30 infections. In other mice inoculated with 1088-N4#14, the patterns were varied, with some similar to the 1088 (N0) infections and some similar to the 1088-N30 infections (Supplementary Fig. 2). The results for the 1088-N4#14 infection seem to represent a rate of lethality of 50%.

We also checked the VNA titer in serum of the infected mice because the response is important for the clearance of rabies virus (Hooper et al., 1998, 2009). At 5 days p.i. when viral antigens were detected in the cortex, the VNA titer was significantly higher in mice infected with 1088 variants compared to 1088 (N0)-infected mice (Fig. 4B). All mice infected with 1088-N4#14 and four of five mice infected with 1088-N30 had a VNA titer of more than 0.5 IU/ml, the criterion for preventing rabies (World Health Organ, 2005), whereas only one of five mice infected with 1088 (N0) had a VNA titer of more than 0.5 IU/ml. The tendency for the variants to induce a greater response than 1088 (N0) was also observed at 8 and 11 days p.i., although all of the mice infected with 1088 (N0) had a VNA titer above 0.5 IU/ml.

Table 2
Pathogenicity of 1088 (N0) and 1088 variants in adult mice after i.m. inoculations.

Dose (FFU)	No. dead/no. tested		
	1088 (N0)	1088-N4#14	1088-N30
10^6	10/10	5/10	0/10
10^5	7/10	5/10	1/10
10^4	8/10	0/10	3/10
10^3	5/10	2/10	1/10
Total	30/40	12/40	4/40

3.8. Kinetics of virus entry into NA cells

In the case of SHBRV-18, efficient internalization into NA cells is responsible for the neruroinvasiveness (Faber et al., 2004). As shown above, however, the 1088 variants were still neuroinvasive. Not surprisingly, no obvious differences were observed in internalization efficiency between the three viruses (Fig. 5).

3.9. Low-pH-dependent fusion of the G protein in transfected cells

Faber et al. (2005) have demonstrated that position 194 of the G protein is related to the pathogenicity of the virus and a mutation at this position affects the pH threshold for membrane fusion by the G protein. We assessed the pH-dependent cell fusion in NA cells by transfection of the G expression vector (Fig. 6). At pH 6.0, cell fusion was observed in most NA cells transfected with the plasmid encoding the G protein of 1088 (N0) or 1088-N4#14 (R196S mutation), whereas fused cells were rarely recognized in the 1088-N30 G (P144L and R196S mutations) transfection. Cell fusion was observed clearly in the cells transfected with the G protein of 1088-N30 at pH 5.8, but rarely recognized in any G transfection at pH 6.2. Hence, the pH threshold of the G protein of 1088-N30 was lower than that of pH compared to the G protein of 1088 (N0) or 1088-N4#14.

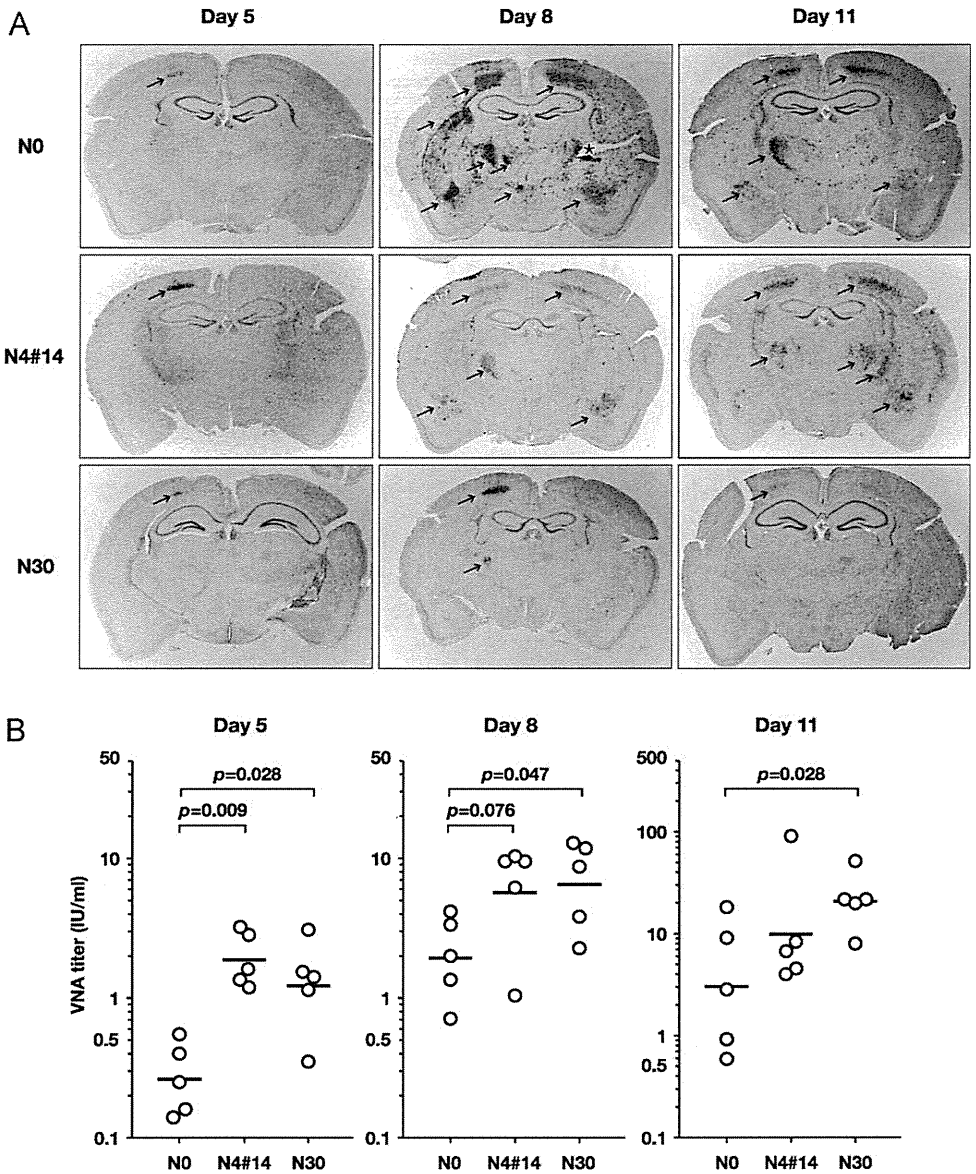

Fig. 4. Mice (15 per group) were inoculated with 1088 (N0), 1088-N4#14 (N4#14), or 1088-N30 (N30) via the i.m. route at 10^6 FFU. At 5, 8 and 11 days p.i., 5 mice per group were sacrificed and their sera, tissues, and organs were sampled. (A) Immunohistochemical analysis of viral antigens in the inoculated mouse brain at different time points. Coronal sections of the mouse brain were stained with anti-P serum. Each image is representative of five individual mice at each time point. Arrows indicate P-protein-positive cells. The asterisk indicates an artifact. (B) VNA responses in the mice. VNA titers were determined by RFFIT and represented as IU/ml. Each open circle in the graphs shows a VNA titer in individual mouse serum. All mock-injected mice showed <0.2 IU/ml (data not shown). Bars represent geometric means. *P* values in the graphs were determined by Mann–Whitney's *U* test. Only *P* values less than 0.1 were indicated.

4. Discussion

Parasites, including viruses, are generally attenuated in an original host during serial passage in a new host (e.g., cell cultures), in part because of a loss of pathogenicity due to the accumulation of deleterious mutations (Ebert, 1998). Current fixed rabies virus strains have been established by serial passage of street viruses in animal brains, tissues and/or cell lines. Most fixed viruses show a reduction or loss of pathogenesis on inoculation via peripheral sites although they are still neurovirulent. Pathogenicity on infection via peripheral sites is one of the phenotypes characterizing street viruses. Since pathogenicity is important to the transmission and circulation of rabies viruses in nature but not under laboratory conditions, the fixed viruses have lost the ability presumably because mutations have emerged and become fixed during serial passaging due to the absence of negative selection. Interestingly, it was demonstrated that attenuated fixed viruses reverted to neurovirulent after a few passages in neuroblastoma cell lines (Clark, 1978). Therefore, we speculated that neurovirulence is maintained during serial passaging in neuroblastoma cells but the phenotype(s) specific to street viruses is not. Hence, we performed the serial passage of street virus 1088 in mouse neuroblastoma NA cells and succeeded in establishing a variant, 1088-N30, which was attenuated in mice after i.m. but not i.c. inoculations.

Most fixed viruses have three or four potential glycosylation sites on the G protein, and two sequons at Asn^{37} and Asn^{319} are common in fixed viruses (Morimoto et al., 1992). The sequon at Asn^{319} is conserved in all known lyssaviruses (Badrane and Tordo, 2001), and the sequon at Asn^{37} is not efficiently glycosylated (Shakin-Eshleman et al., 1992). Ming et al. (2009) mentioned that several street viruses lack the sequon at Asn^{247} observed in several fixed viruses. Indeed, street viruses whose entire genome has been sequenced possess one or two potential *N*-glycosylation sites in the G protein (as summarized in Table 3). Moreover, most of

Table 3
Potential *N*-glycosylation sites on the G protein of street and fixed rabies viruses.

Strain	Origin	Location	Year	*N*-Glycosylation sites (potential[a])	GenBank accession no.	Ref.
Street viruses						
1088	Woodchuck	USA	1970s	37, 319	AB645847	This work
BR-Pfx1	Fox	Brazil	2002	37, 319	AB362483	Mochizuki et al. (2009)
HN10	Human	China	2006	37, 319	EU643590	Ming et al. (2009)
NNV-RAB-H	Human	India		37, 319	EF437215	Nagaraja et al. (2008)
H-08-1320	Human	Sri Lanka	2008	37, 319	AB569299	Matsumoto et al. (2011)
8743THA[b]	Human	Thailand	1983	37, 319	EU293121	Delmas et al. (2008)
8764THA	Human	Thailand	1983	37, 319	EU293111	Delmas et al. (2008)
9001FRA	Dog[c]	French Guyana	1991	37, 319	EU293115	Delmas et al. (2008)
9147FRA	Fox	France	1990	37, 319	EU293113	Delmas et al. (2008)
9704ARG	Bat	Argentina	1997	319	EU293116	Delmas et al. (2008)
RRV ON-99-2	Raccoon	USA	1999	319	EU311738	Szanto et al. (2008)
SHBRV-18	Bat	USA		237, 319	AY705373	Faber et al. (2004)
Fixed viruses						
CVS-11				37, 204, 319	EU352767	Wright et al. (2008)
Pitman Moore	Vaccine			37, 204, 319	AJ871962	
ERA	Vaccine			37, 247, 319	EF206707	Geue et al. (2008)
SAD B19	Vaccine			37, 247, 319	M31046	Conzelmann et al. (1990)
RV-97	Vaccine			37, 247, 319	EF542830	Metlin et al. (2008)
Nishigahara	Vaccine			37, 247, 319	AB044824	Ito et al. (2001a)
RC-HL	Vaccine			37, 247, 319	AB009663	Ito et al. (2001a)
PV	Vaccine			37, 158, 247, 319	M13215	Tordo et al. (1986)
HEP-Flury	Vaccine			37, 158, 319	M32751	Morimoto et al. (1989)

[a] Sequons in ectodomain.
[b] Passaged 22 times in BSR cells.
[c] Bitten by a bat.

the G sequences of field isolates available in GenBank also possess only one or two potential *N*-glycosylation sites (Asn^{319}, or Asn^{37} and Asn^{319}), although the SHBRV-18 G protein has sequons at Asn^{237} and Asn^{319}. Thus, it is likely that the *N*-glycosylation of the G protein is strictly subjected to the pressures of natural selection because there is some disadvantage for street viruses. In the present study, we found that the G protein of 1088 (N0) possesses only two potential *N*-glycosylation sites, at Asn^{37} and Asn^{319}, whereas 1088-N30 has three sites as well as fixed strains. In order to demonstrate that the additional *N*-glycosylation affects the phenotype(s) of the street virus, we attempted to select a cloned variant that has the *N*-glycosylation mutation only. Although, unfortunately, we could not obtain such a variant, we selected 1088-N4#14, which has another mutation in addition to the *N*-glycosylation mutation. We found that 1088-N4#14 and 1088-N30 were less pathogenic in adult mice than the parental 1088 after i.m. inoculations, although 1088-N4#14 was not highly attenuated. The reduced pathogenicity in the i.m. infection, even if not highly attenuated, would affect viral transmission and circulation. The mutation in the P protein of 1088N4#14 (Glu at position 61) is also found in several street virus strains, indicating that it is not likely to impair the pathogenesis. Therefore, the additional *N*-glycosylation is likely involved in the reduced pathogenicity though it is not the sole determinant of the attenuated phenotype of 1088-N30. Consequently, we think that under natural conditions, the street virus population in which the mutation leading to additional *N*-glycosylation has arisen may be negatively selected.

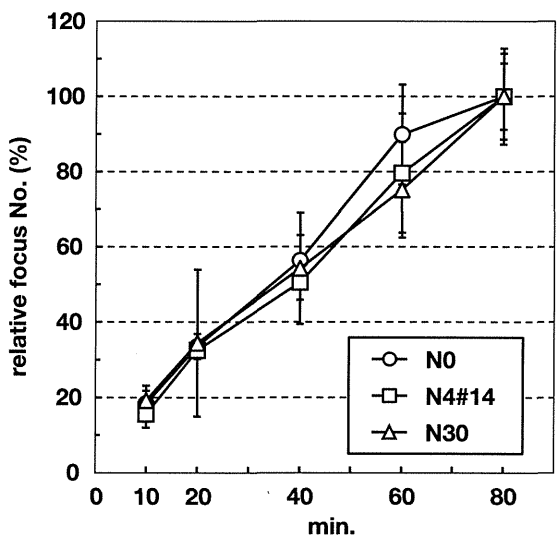

Fig. 5. Efficiency of virus internalization in NA cells. The same titer of virus was added to each well and then incubated for the period indicated at 37 °C. After incubation, the cells were washed and overlaid with medium containing methylcellulose. Viral foci derived from internalized viruses were visualized at 4 days p.i. and the internalization efficiency of each strain is indicated as the relative number of foci, taking the number at 80 min as 100%. Values represent the mean ± SD from four individual wells.

We found a correlation between the attenuation of 1088-N30 and induction of a humoral immune response. It is likely that the induction of a strong immune response is one of the factors responsible for the attenuation of 1088-N30. The highly restricted spread of 1088-N30 in the CNS after the i.m. inoculation is probably due to a strong immune response rather than a loss of ability for neuron-to-neuron spread, because 1088-N30 was still pathogenic after the i.c. inoculation. Indeed, the street virus strain SHBRV induced weak innate immune responses compared with an attenuated fixed virus (Wang et al., 2005). Several lines of evidence indicate that immune evasion of street viruses is important for pathogenicity through the maintenance of the BBB's integrity to prevent immune effectors entering the CNS (Kuang et al., 2009; Roy and Hooper, 2007, 2008; Roy et al., 2007). From our results, although the possibility that the G protein with the additional *N*-glycosylation had enhanced immunogenicity itself could not be ruled out, the marked enhancement of virus production is a rational explanation for the induction of the strong immune response.

Interestingly, Faber et al. (2005) reported that the Asn residue at position 194 of the G protein is related to pathogenicity. On comparing two Asn^{194} mutants, one virulent and one avirulent, they found that the virulent mutant showed enhanced internalization

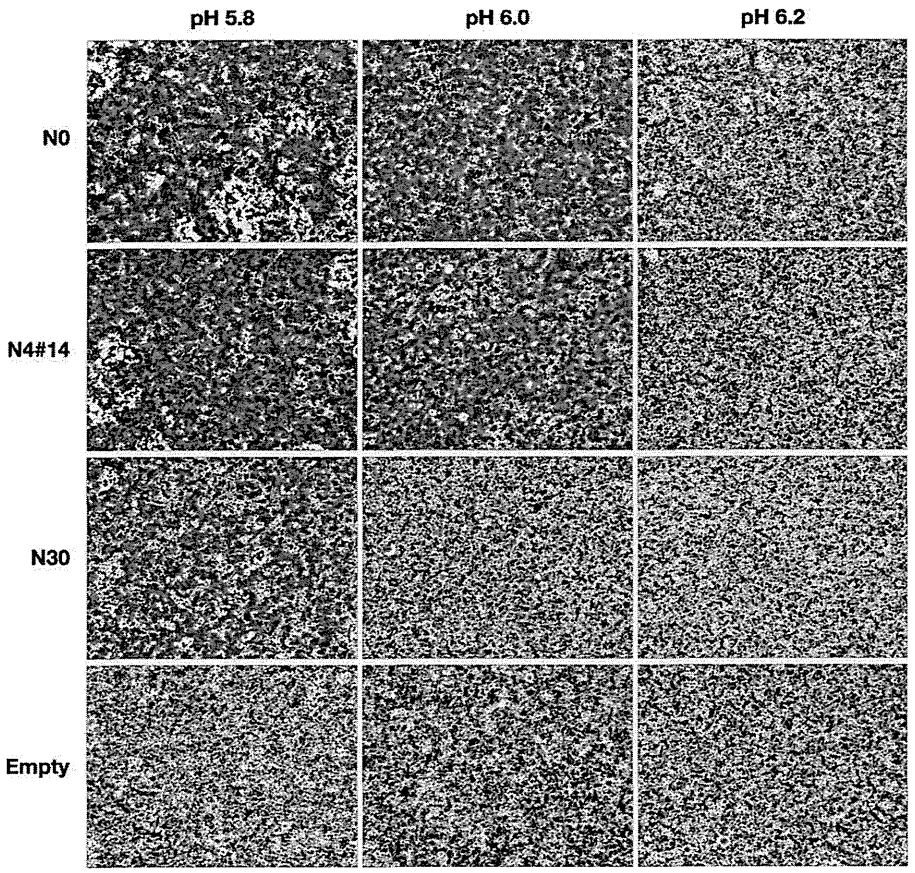

Fig. 6. Low-pH cell fusion by the G protein. NA cells were transfected with a plasmid encoding the G protein of 1088 (N0), 1088-N4#14 (N4#14), or 1088-N30 (N30). Empty vector was also transfected. At 2 days after the transfection, the cells were treated with fusion medium at the indicated pH and incubated at 37 °C for 30 min. Fused cells were stained with fuchsine solution.

efficiency in cells, enhanced cell-to-cell spread, and a higher pH threshold of membrane fusion activity by the G protein. Therefore, the *N*-glycosylation at Asn^{194} was likely to affect these characteristics. However, we did not detect a difference in internalization efficiency and pH threshold between the parental 1088 and 1088-N4#14 (Figs. 5 and 6). Furthermore, contrary to their result, the 1088 variants made larger foci than the parental strain in NA cells (our unpublished observation). Hence, the mechanism of attenuation via *N*-glycosylation at Asn^{194} is different from that via the mutation at position 194 without *N*-glycosylation reported previously.

Although 1088-N4#14 induced a humoral immune response as strongly as did 1088-N30, it exhibited intermediate pathogenicity between that of 1088 (N0) and 1088-N30. The other mutations are also probably related to the greater attenuation. Prehaud et al. (1988) demonstrated that one escape mutant of the CVS strain selected with a MAb against antigenic site II of the G protein was 300 times less pathogenic than the parental CVS after i.m. inoculation. The mutant had an amino acid mutation at position 147. The region around position 147 including position 144 is also likely important to the pathogenicity. Indeed, we found that the 1088-N30 G protein (P144L and R196S mutations), but not the 1088-N4#14 G protein (R196S mutation), had a lower pH threshold of membrane fusion activity than the G protein of 1088. As described above, Faber et al. (2005) demonstrated a correlation between a lower pH threshold and attenuation. Therefore, the P144L mutation might be more closely related to the attenuated phenotype of 1088-N30 than the R196S mutation. In addition, since the Pro at position 144 is absolutely conserved among the G proteins deposited in GenBank (our unpublished observation), position 144 is probably important to the pathogenicity of the street viruses.

Mutations in the leader and trailer sequences (nt 17, 28, and 11870), and N protein (E373E/K) of 1088-N30 also have the potential to be involved in the greater attenuation. Indeed, Faber et al. (2004) reported that the trailer sequence could modulate the pathogenicity of SHBRV, and the involvement of leader and trailer sequences in the viral pathogenesis has also reported in other *Mononegavirales* (Banyard et al., 2005; Fujii et al., 2002). On the other hand, Masatani et al. (2010) demonstrated that the N protein of a pathogenic fixed strain functioned to evade retinoic acid-inducible gene I (RIG-I)-mediated antiviral responses but that of an attenuated strain did not. Therefore, the attenuated strain strongly activated expression of interferon and chemokine genes in infected cells. They also reported that amino acids at positions 273 and 394 of the N protein are important for the evasion and pathogenesis (Masatani et al., 2011). Intriguingly, the latter is located near the mutation detected in the N gene of 1088-N30.

We cannot rule out the possibility that the mutation detected in the P protein of 1088-N4#14 disguises the attenuating effects of the R196S mutation. The Glu residue at position 61 of the P protein was also detected in several field isolates from terrestrial animals, the sequences of which are available in GenBank. Therefore, it is possible that the mutation enhances rather than impairs the pathogenicity as mentioned above. It has been demonstrated that the P protein functions to interfere with the interferon system (Brzozka et al., 2005, 2006; Ito et al., 2010; Rieder et al., 2011; Vidy et al., 2005) and interact with dynein light chain LC8 (Jacob et al., 2000; Raux et al., 2000). The interaction is slightly related to

the pathogenicity (Mebatsion, 2001; Rasalingam et al., 2005). However, position 61 is outside of the domains identified as important for functions.

Both 1088 variants showed much better proliferative activity than the parental 1088 in NA cells. Therefore, the additional *N*-glycosylation, common mutation to both variants, is likely responsible for the adaptation. It seems that the additional *N*-glycosylation enhanced the release of viral particles from the cells, since the expression levels of viral proteins were similar between 1088 (N0) and 1088-N4#14 at an MOI of 1 (Fig. 3B). Interestingly, in the case of WNV, the *N*-glycosylated E protein enhanced the viral replication efficiency in cell lines (Beasley et al., 2005; Li et al., 2006; Shirato et al., 2004), and WNV whose E protein was glycosylated budded from the cell surface but the non-glycosylated variant budded at intracellular membranes (Li et al., 2006). This is also likely in the present case. Several ultrastructural studies have demonstrated that street viruses matured by budding at intracellular membranes, such as the endoplasmic reticulum (ER), but fixed viruses preferred to bud from the plasma membrane in cultured neural cells and within the CNS (Fekadu et al., 1982; Iwasaki et al., 1975; Iwasaki and Tobita, 2002; Matsumoto et al., 1974; Matsumoto and Yonezawa, 1971; Murphy et al., 1973). The mechanism by which the additional *N*-glycosylation of the G protein enhances viral production should be elucidated by further investigation.

While 1088-N30 showed strong growth in NA cells, its G protein was expressed at a lower level than that of 1088 (N0) or 1088-N4#14 (Fig. 3B). A similar result was found in Fig. 2A. This was not due to the sensitivity of the anti-G MAb 15-13, because the 1088-N30 G protein was detected at the same level as the 1088 (N0) and 1088-N4#14 G proteins by this MAb when the G proteins were expressed using a plasmid vector (Fig. 2B). Moreover, the MAb 15-13 recognizes a linear epitope containing the amino acid at position 251 of the G protein (Luo et al., 1997). Furthermore, the G mRNA levels of 1088-30 were similar to those of 1088 (N0) and 1088-N4#14 (Supplementary Fig. 1). Therefore, the low expression of the G protein of 1088-N30 was due to post-transcriptional events in the infected cells. Generally, newly synthesized glycoproteins undergo proper folding by chaperons in the ER, whereas misfolded proteins are eliminated via the ER-associated degradation (ERAD) pathway, in which misfolded proteins are retrotranslocated from the ER to the cytoplasm and then degraded by the proteasome (Ruddock and Molinari, 2006). It was reported that the hepatitis C virus activates the ERAD pathway and that the half-life of viral glycoproteins in infected cells increased when ERAD was inhibited (Saeed et al., 2011). Thus, the ERAD pathway might be activated in the 1088-N30-infected cells but not 1088 (N0)- or 1088-N4#14-infected cells, or the 1088-N30 G protein might be more easily degraded under conditions in which ERAD is facilitated. In addition, the reason why 1088-N30 multiplied efficiently in NA cells in spite of low levels of the G protein might be that the G protein's expression is not a rate-determining factor for viral production in 1088-N30-infected NA cells.

In this study, by comparing strains with different virulence but with very similar genomic sequences, we could discuss the viral elements related to the pathogenicity of street viruses at the nucleotide and amino acid levels. Then, we found a relationship between the *N*-glycosylation of the rabies virus G protein and biological activities such as growth ability and pathogenicity. Database analysis suggests that the number of *N*-glycosylation sites in the G protein is limited in field isolates, and is probably under natural selection. In support of this, our results indicate that the additional *N*-glycosylation might interfere with the pathogenicity required for circulation in nature, although it is an adaptive mutation in NA cells. However, since the *N*-glycosylation at Asn^{194} is novel in the rabies virus and 1088-N4#14 has another mutation, it should be confirmed whether the additional *N*-glycosylation at Asn^{194} is solely responsible for the attenuation of 1088 and other street strains. Generalizing the concept presented here would be one way to facilitate understanding of the pathogenicity of rabies viruses. For this, further investigation is required to assess whether the additional *N*-glycosylation observed in fixed viruses (at Asn^{158}, Asn^{204}, or Asn^{247}) also affects the pathogenicity of street viruses.

Acknowledgements

We thank Dr. M. Sugiyama (Gifu University, Gifu, Japan) for providing the anti-G MAb 15-13.

This study was supported in part by grants from the Ministry of Education, Culture, Sports, Science and Technology of Japan (no. 21780278) and from the Ministry of Health, Labour and Welfare of Japan.

Appendix A. Supplementary data

Supplementary data associated with this article can be found, in the online version, at doi:10.1016/j.virusres.2012.01.002.

References

Badrane, H., Tordo, N., 2001. Host switching in Lyssavirus history from the Chiroptera to the Carnivora orders. J. Virol. 75, 8096–8104.
Baer, M.G., 2007. The history of rabies. In: Jackson, A.C., Wunner, W.H. (Eds.), Rabies. , 2nd ed. Academic Press, San Diego, pp. 1–22.
Banyard, A.C., Baron, M.D., Barrett, T., 2005. A role for virus promoters in determining the pathogenesis of Rinderpest virus in cattle. J. Gen. Virol. 86, 1083–1092.
Beasley, D.W., Whiteman, M.C., Zhang, S., Huang, C.Y., Schneider, B.S., Smith, D.R., Gromowski, G.D., Higgs, S., Kinney, R.M., Barrett, A.D., 2005. Envelope protein glycosylation status influences mouse neuroinvasion phenotype of genetic lineage 1 West Nile virus strains. J. Virol. 79, 8339–8347.
Brzozka, K., Finke, S., Conzelmann, K.K., 2005. Identification of the rabies virus alpha/beta interferon antagonist: phosphoprotein P interferes with phosphorylation of interferon regulatory factor 3. J. Virol. 79, 7673–7681.
Brzozka, K., Finke, S., Conzelmann, K.K., 2006. Inhibition of interferon signaling by rabies virus phosphoprotein P: activation-dependent binding of STAT1 and STAT2. J. Virol. 80, 2675–2683.
Clark, H.F., 1978. Rabies viruses increase in virulence when propagated in neuroblastoma cell culture. Science 199, 1072–1075.
Conzelmann, K.K., Cox, J.H., Schneider, L.G., Thiel, H.J., 1990. Molecular cloning and complete nucleotide sequence of the attenuated rabies virus SAD B19. Virology 175, 485–499.
Delmas, O., Holmes, E.C., Talbi, C., Larrous, F., Dacheux, L., Bouchier, C., Bourhy, H., 2008. Genomic diversity and evolution of the lyssaviruses. PLoS One 3, e2057.
Dietzschold, B., Morimoto, K., Hooper, D.C., Smith, J.S., Rupprecht, C.E., Koprowski, H., 2000. Genotypic and phenotypic diversity of rabies virus variants involved in human rabies: implications for postexposure prophylaxis. J. Hum. Virol. 3, 50–57.
Dietzschold, B., Wiktor, T.J., Trojanowski, J.Q., Macfarlan, R.I., Wunner, W.H., Torres-Anjel, M.J., Koprowski, H., 1985. Differences in cell-to-cell spread of pathogenic and apathogenic rabies virus in vivo and in vitro. J. Virol. 56, 12–18.
Dietzschold, B., Wunner, W.H., Wiktor, T.J., Lopes, A.D., Lafon, M., Smith, C.L., Koprowski, H., 1983. Characterization of an antigenic determinant of the glycoprotein that correlates with pathogenicity of rabies virus. Proc. Natl. Acad. Sci. U. S. A. 80, 70–74.
Ebert, D., 1998. Experimental evolution of parasites. Science 282, 1432–1435.
Etessami, R., Conzelmann, K.K., Fadai-Ghotbi, B., Natelson, B., Tsiang, H., Ceccaldi, P.E., 2000. Spread and pathogenic characteristics of a G-deficient rabies virus recombinant: an in vitro and in vivo study. J. Gen. Virol. 81, 2147–2153.
Faber, M., Faber, M.L., Papaneri, A., Bette, M., Weihe, E., Dietzschold, B., Schnell, M.J., 2005. A single amino acid change in rabies virus glycoprotein increases virus spread and enhances virus pathogenicity. J. Virol. 79, 14141–14148.
Faber, M., Pulmanausahakul, R., Nagao, K., Prosniak, M., Rice, A.B., Koprowski, H., Schnell, M.J., Dietzschold, B., 2004. Identification of viral genomic elements responsible for rabies virus neuroinvasiveness. Proc. Natl. Acad. Sci. U. S. A. 101, 16328–16332.
Fekadu, M., Chandler, F.W., Harrison, A.K., 1982. Pathogenesis of rabies in dogs inoculated with an Ethiopian rabies virus strain. Immunofluorescence, histologic and ultrastructural studies of the central nervous system. Arch. Virol. 71, 109–126.
Fujii, Y., Sakaguchi, T., Kiyotani, K., Huang, C., Fukuhara, N., Egi, Y., Yoshida, T., 2002. Involvement of the leader sequence in Sendai virus pathogenesis revealed by recovery of a pathogenic field isolate from cDNA. J. Virol. 76, 8540–8547.
Geue, L., Schares, S., Schnick, C., Kliemt, J., Beckert, A., Freuling, C., Conraths, F.J., Hoffmann, B., Zanoni, R., Marston, D., McElhinney, L., Johnson, N., Fooks, A.R., Tordo, N., Muller, T., 2008. Genetic characterisation of attenuated. SAD rabies virus strains used for oral vaccination of wildlife. Vaccine 26, 3227–3235.